



Magnetostratigraphy, nannofossil stratigraphy and apparent polar wander for Adria-Africa in the Jurassic–Cretaceous boundary interval

J.E.T. Channell ^{a,*}, C.E. Casellato ^b, G. Muttoni ^b, E. Erba ^b

^a Department of Geological Sciences, University of Florida, Gainesville, FL 32611, USA

^b Dipartimento di Scienze della Terra "A.Desio", Università degli Studi di Milano, via Mangiagalli 34, 20133 Milano, Italy

ARTICLE INFO

Article history:

Received 27 August 2009

Received in revised form 12 April 2010

Accepted 26 April 2010

Available online 6 May 2010

Keywords:

Late Jurassic

Jurassic/Cretaceous boundary

Polarity chron

Calcareous nannofossils

Apparent polar wander path

Paleolatitudes

ABSTRACT

Existing correlations of Early Cretaceous nannofossil events to polarity zones in Italian pelagic limestones are the basis for correlation of polarity chronos to geologic stages, and hence calibration of the Early Cretaceous geomagnetic polarity timescale. Here, we present correlations of nannofossil events to polarity chronos for the Late Jurassic and Jurassic/Cretaceous boundary interval from the Southern Alps, making the case for revisions of current geologic timescales in this interval. The Jurassic/Cretaceous and Kimmeridgian/Tithonian boundaries can be usefully defined at the onsets of polarity chronos CM18R and CM22R, respectively. The Oxfordian/Kimmeridgian boundary can be assigned to CM25. An apparent polar wander path (APWP) for the Southern Alps, derived from, and time-calibrated by bio-magnetostratigraphic data, is similar to, and provides a proxy for, the African APWP in the absence of adequate African data of this age. The Southern Alpine APWP is characterized by a cusp (hairpin) at ~30°N/270°E at a time close to the Oxfordian/Kimmeridgian boundary (polarity chron CM25, ~154 Ma), rapid APWP from high latitude (>60°N) in the preceding middle Jurassic (Bajocian-Oxfordian) interval coincident with the onset of Central Atlantic/Ligurian oceanic rifting, and a return to high latitudes during the Cretaceous. Early Jurassic poles at high latitudes (>60°N) are evident for Sinemurian to Toarcian-Aalenian time (175–195 Ma). An APWP for this time interval with this level of temporal calibration cannot be constructed using data from Africa itself, or from other Atlantic-bordering continents by rotation to African coordinates.

© 2010 Elsevier B.V. All rights reserved.

1. Introduction

The continental margin exposed in the Southern Alps was formed at the time of Early–Middle Jurassic rifting that shaped the Ligurian Ocean between Adria (Africa) and Europe. The Ligurian Ocean was contiguous with, and initiated at the same time as, the Central Atlantic between Adria and Europe (Bernoulli and Jenkyns, 1974; Bosellini, 2004; Bernoulli and Jenkyns, 2009). Adria, the continental crust centered on the Adriatic Sea and including the surrounding deformed continental margins, has been considered as a promontory of the African plate since the Late Paleozoic (e.g. Channell et al., 1979a; Channell, 1996; Muttoni et al., 2001, 2003). Jurassic extension of the continental margin gave rise to a series of platforms and basins from the internal (oceanward) Lombardian Basin to the external Friuli-Dinaric Platform (Fig. 1). The exposed Upper Jurassic–Lower Cretaceous sedimentary succession in the Southern Alps provides a classic example of an exposed passive margin (see Winterer and Bosellini,

1981). Although Late Cenozoic deformation and thrusting affected the entire region, the relatively low level of deformation and the lack of metamorphism in the Mesozoic sedimentary succession make the area an ideal laboratory for sedimentary, biostratigraphic and structural studies.

The region has also been a focus of Early Cretaceous biostratigraphic studies, particularly the study of nannofossils, calpionellids and their correlation to polarity zones (e.g. Channell et al., 1979b, 1987, 1993; Erba and Quadrio, 1987; Channell and Erba, 1992; Erba et al., 1999). These early studies formed a basis for the correlation of polarity chronos to geologic stages in this time interval (see review by Channell et al., 1995a, 2000). The focus of this paper is the magneto-biostratigraphy of the Kimmeridgian to Berriasian interval spanning the Jurassic/Cretaceous (J/K) boundary. This interval is characterized by biostratigraphically and environmentally significant nannofossil and calpionellid evolution and by a marked cusp (hairpin) in the apparent polar wander path (APWP) of Adria. Due to the continuity of the African Mesozoic continental margin into Adria, the apparent match of the Mesozoic APWPs of Adria and Africa, and the relative paucity of African data of this age, the Adria APWP has been considered applicable to Africa (e.g. Channell, 1996; Muttoni et al., 2001). The magneto-biostratigraphy presented here provides a means of calibrating this intriguing segment of the Adria-Africa APWP.

* Corresponding author. Tel.: +1 352 3923658; fax: +1 352 3929294.

E-mail address: jetc@ufl.edu (J.E.T. Channell).

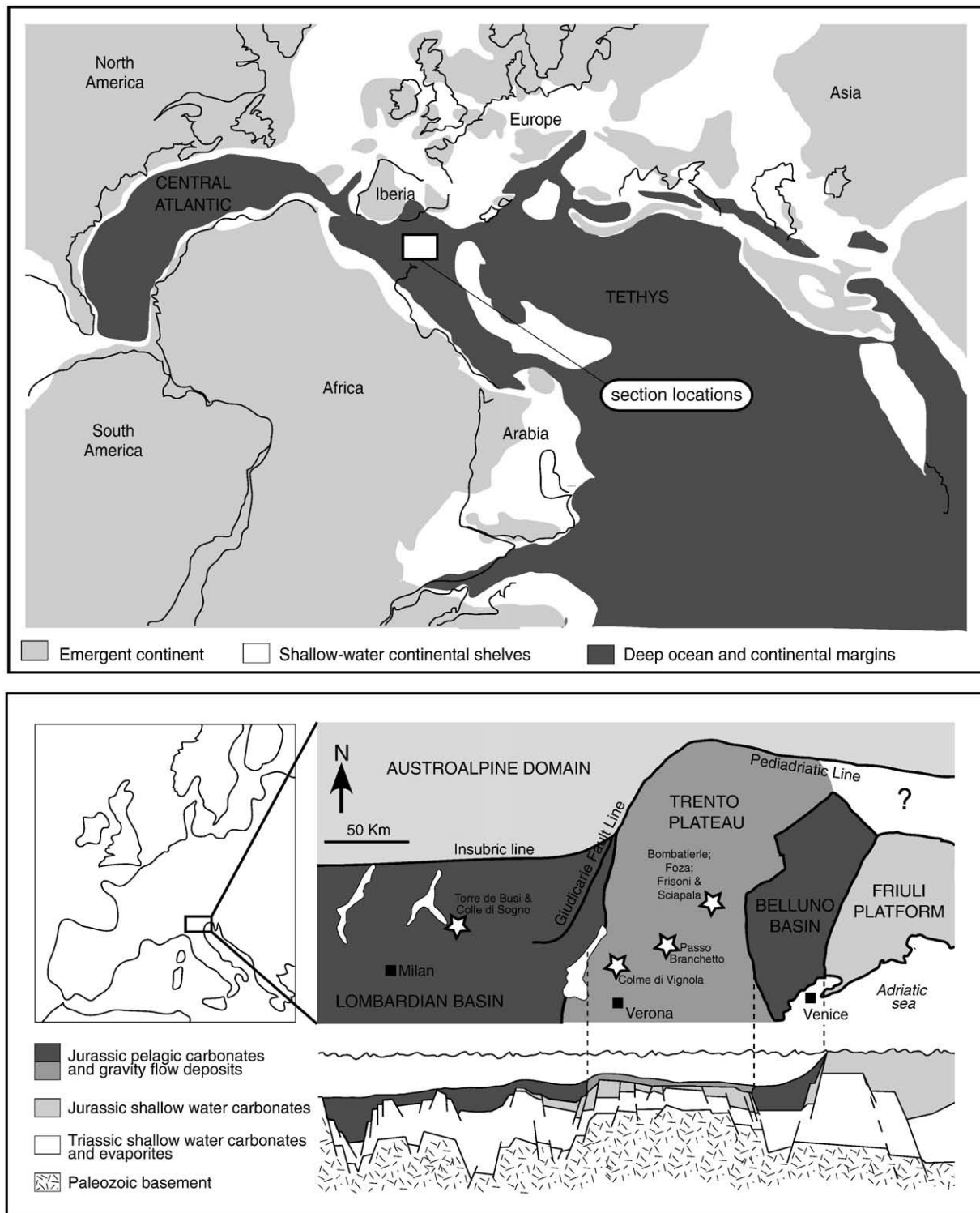


Fig. 1. Paleogeographic map for Callovian–Oxfordian time (after Barrier and Vrielynck, 2008) and schematic paleogeographic cross-section of the Southern Alps (northern Italy), for latest Jurassic time (after Winterer and Bosellini, 1981) showing locations of sedimentary sections sampled for this study.

2. Sampling sites

The sampling sites are in the central part of the Lombardian Basin and on the Trento Plateau (Fig. 1). The sites in the Lombardian Basin are located on the road leading northward from the village of Torre de' Busi to Colle di Sogno, a vantage point overlooking the town of Lecco on Lake Como. Well-exposed road outcrops comprise a virtually continuous

section straddling almost the entire Jurassic from the Lower Jurassic Calcare di Moltrasio to the Maiolica Formation that spans the J/K boundary. Eleven paleomagnetic sampling sites were collected in this Jurassic section by Muttoni et al. (2005), who found low (~10°N) paleolatitudes in Middle to early Late Jurassic radiolarian-bearing cherts (Radiolariti) that were associated with continental drift into a near-equatorial upwelling zone of high biosiliceous productivity.

For this paper, two sections were sampled for magnetostratigraphy along the road from the village of Torre de' Busi to Colle di Sogno. The Torre de' Busi section (at 45° 46' 34" N, 9° 29' 7" E) is located 3 km north of the village of the same name. The studied 60 m-thick section comprises a road cut exposing the uppermost part of the red Radiolariti, the Rosso ad Aptici and the lowermost Maiolica Formation (Figs. 2 and 3). Following the same road up-hill for about 10 km to the crest of the Monte Brughetto, the studied "Colle di Sogno" section comprises a 350 m-thick succession of pelagic and hemipelagic limestones and marlstones (Fig. 4). The lower part of the section (at 45° 47' 29" N, 9° 28' 44" E) includes the Sinemurian–Pliensbachian Calcare di Moltrasio and Calcare di Domaro formations, which are overlain by the Toarcian–Aalenian Sogno Formation. The very regular decimeter-scale bedding that characterizes the Calcare di Domaro has been interpreted as

having been produced by orbital forcing (Hinnov and Park, 1999; Hinnov et al., 2000).

The other sampled sections are located on the Trento Plateau. The Colme di Vignola section (at 45° 45' 58" N, 10° 57' 20" E) lies above the village of Brentonico on the slopes of Monte Vignola, at the western margin of the Trento Plateau (Fig. 1). The studied 20 m-thick section spans the Calcare Selcifero di Fonza, the Rosso Ammonitico Superiore, and the lowermost part of the Biancone (the local Maiolica equivalent) (Fig. 5). Four other sections (Foza, Frisoni, Sciapala and Bombatierle; Fig. 1) are located on the Trento Plateau within 20 km of the town of Asiago. The Foza section (45° 53' 44" N, 11° 36' 3" E), first described by Ogg (1981), and referred to as the Val Miela section by Ogg et al. (1991) and Martire (1996), lies between the villages of Foza and Gallio (east of Asiago) and provides excellent exposure of the

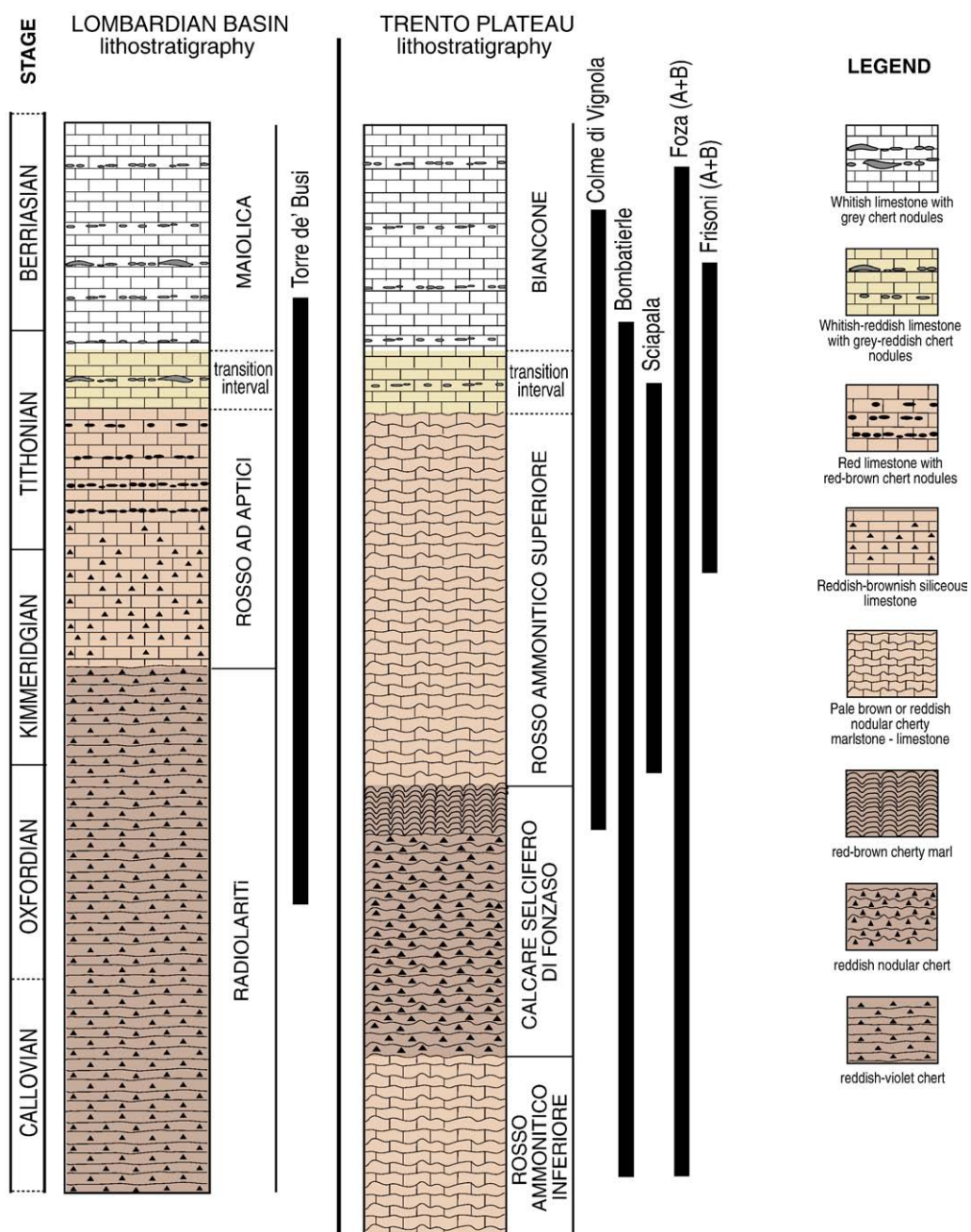


Fig. 2. Schematic Callovian to Berriasian (Middle Jurassic to Early Cretaceous) lithostratigraphy of the Lombardian Basin and Trento Plateau, northern Italy (after Baumgartner et al., 2001).

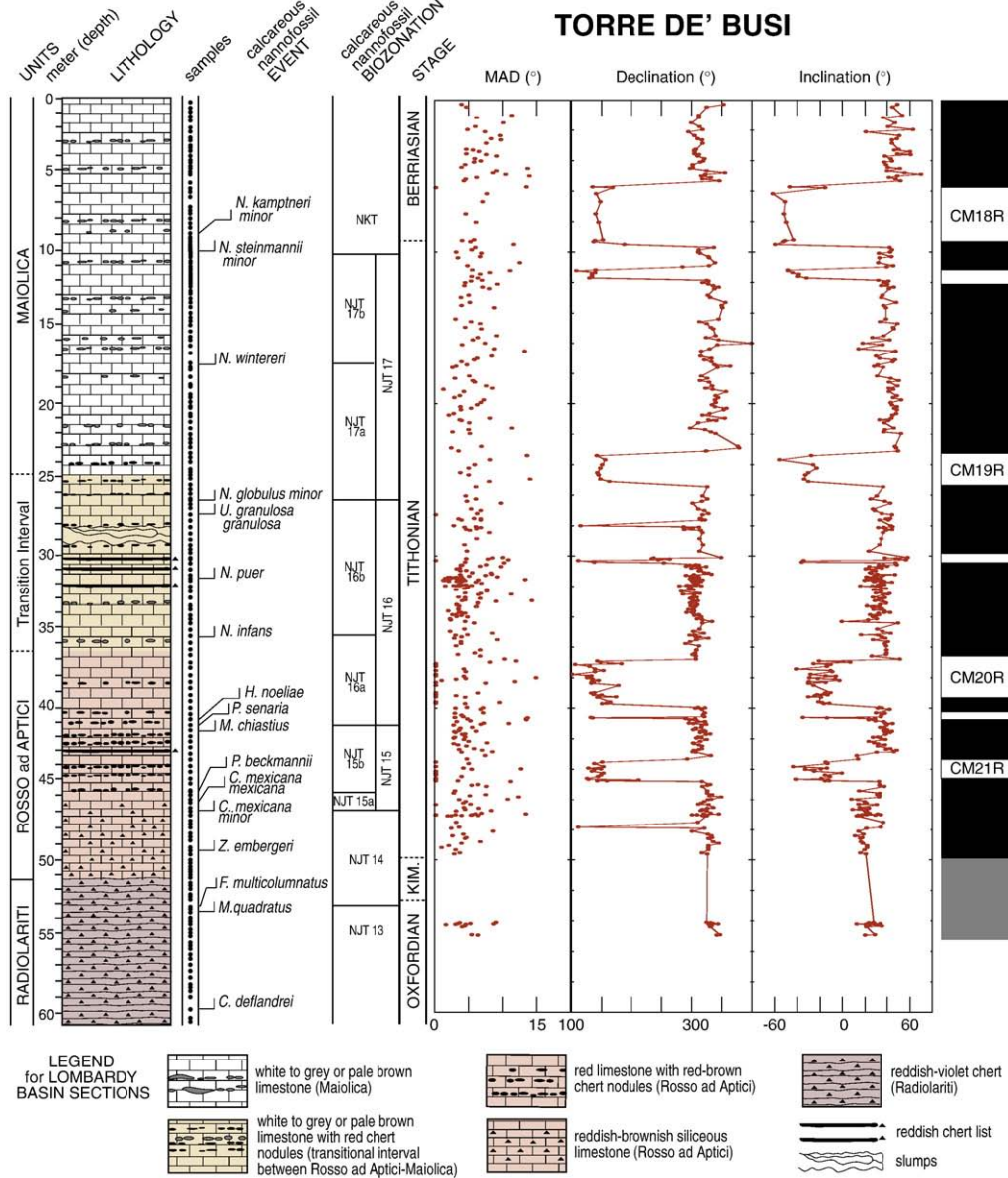


Fig. 3. The lithostratigraphy, biostratigraphy and magnetostratigraphy of the Torre de' Busi section. Component declination and inclination, with maximum angular deviation (MAD) values, are interpreted in terms of normal (black blocks) and reverse (white blocks) polarity zones.

Rosso Ammonitico Inferiore, the Calcare Selcifero di Fonzaso, the Rosso Ammonitico Superiore and the Biancone limestones (Fig. 6). The studied 47 m-thick section is complemented by partial exposure of the same section around the next bend on the road towards Gallio. This second exposure is designated Foza B, and the primary exposure is referred to as Foza A. The Frisoni sections are located 5 km east of the village of Foza close to the bridge spanning the Valgadena, adjacent to the village of Frisoni. The primary section (Frisoni A at 45° 54' 54" N, 11° 39' 17" E) lies on the SW side of the bridge and spans the Rosso Ammonitico Superiore and its transition into the Biancone limestones (Fig. 7). The section on the NE side of the bridge (Frisoni B at 45° 55' 1" N, 11° 39' 25" E) was only sampled for a part of the Rosso Ammonitico Superiore (Fig. 8). The upper part of the Frisoni B section was previously sampled by Channell and Grandesso (1987) for magnetostratigraphy and capionellid biostratigraphy in the interval spanning polarity chronos CM21–CM16 (Tithonian–Berriasian), although outcrop markings from this early study are no longer visible. Note that, in this paper, we label polarity chronos using a "C" prefix followed by the

label corresponding to the correlative marine magnetic anomaly (see Channell et al., 1995a). The prefix serves to clearly distinguish polarity chronos (time intervals) from marine magnetic anomalies. "N" or "R" may be added at the end of the label to distinguish the normal or reverse polarity part of the polarity chron, and subchrons within a normal or reverse polarity chron may be labelled numerically from the onset of the chron (e.g. CM19N-1r).

The Sciapala section (at 45° 51' 21" N, 11° 34' 42" E) is in a disused quarry located 7 km SE of Asiago with access from the Val di Melago. The studied section spans the transition of the Rosso Ammonitico Superiore to the Biancone limestones (Fig. 9). The Bombatierle section (at 45° 50' 55" N, 11° 30' 25" E) is in an active quarry 1 km south of Monte Kaberlaba, the site of a cable-car station located 5 km south of Asiago. The studied section spans the Rosso Ammonitico Inferiore through the Biancone limestones (Fig. 10). In addition, a 5.5 m-thick section of Calcare Selcifero di Fonzaso was sampled (at 45° 41' 10.5" N, 11° 04' 47" E) close to Passo del Branchetto (Fig. 1), 1.5 km west of the ski resort of San Giorgio.

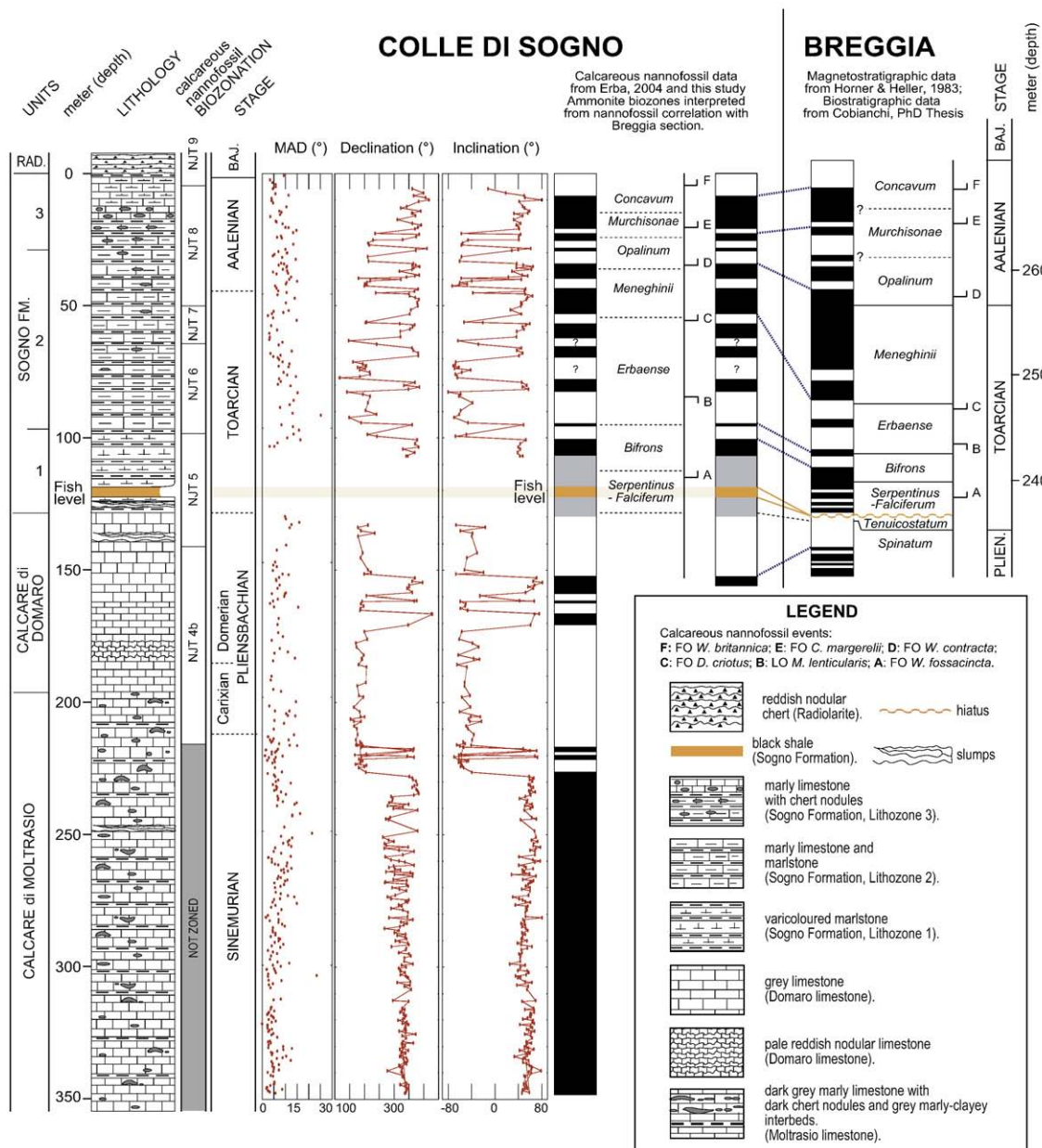


Fig. 4. The lithostratigraphy, biostratigraphy and magnetostratigraphy of the Colle di Sogno section, with correlation to the Breggia section using nannofossil data of Cobianchi (1992) and magnetostratigraphy of Horner and Heller (1983). Component declination and inclination, with maximum angular deviation (MAD) values, are interpreted in terms of normal (black blocks) and reverse (white blocks) polarity zones. Data from Erba (2004).

3. Lithostratigraphy and biostratigraphy

The Mesozoic passive margin exposed in the Southern Alps (Fig. 1) is an example of a Bahamian-type continental margin in which the Lombardian Basin and the Friuli Platform represent the internal (oceanward) and external paleogeographic domains, respectively (Bernoulli and Jenkyns, 1974; Bernoulli et al., 1979; Winterer and Bosellini, 1981; Bosellini, 2004; Bernoulli and Jenkyns, 2009). The stratigraphic ordering of the Upper Jurassic and Lower Cretaceous sedimentary successions (Fig. 2) is based on lithostratigraphic and biostratigraphic studies (Erba and Quadrio, 1987; Baumgartner et al., 2001; Bersezio et al., 2002; Martire et al., 2006; Chiari et al., 2007), and magneto-biostratigraphic studies (Channell et al., 1979b, 1987, 2000; Channell and Grandesso, 1987; Channell and Erba, 1992; Erba et al., 1999). The J/K boundary interval of the Maiolica/Biancone has been well documented, based on calcareous nannofossils, calpionellids, and magnetostratigraphy, both in the Southern Alps and in the Umbria-

Marche Apennines (e.g. Bralower et al., 1989). The Upper Jurassic stratigraphy is less well developed due to discontinuous sedimentation rates, poorer nannofossil preservation, and a lack of appropriate bio-magnetostratigraphic studies.

Nannofossil biostratigraphic zonations for the uppermost Jurassic–Lower Cretaceous have their roots in the work of Thierstein (1971, 1973) who established a nannofossil zonation from successions exposed in southern France. Subsequently, the Lower Cretaceous nannofossil zonation has been revised and correlated to polarity zones in the Umbria–Marche Apennines (Bralower et al., 1989; Channell et al., 1995b) and in the Southern Alps (Channell et al., 1987; Channell and Erba, 1992). The Upper Jurassic nannofossil zonation has also undergone development and revision in the last 20 years (De Kaenel et al., 1996; Bown and Cooper, 1998; Mattioli and Erba, 1999), with further revision by Casellato (submitted for publication). Based on taxonomic revision and improved stratigraphy, the Jurassic Tethyan nannofossil biozones (NJT 1–11) of Mattioli and Erba (1999) have

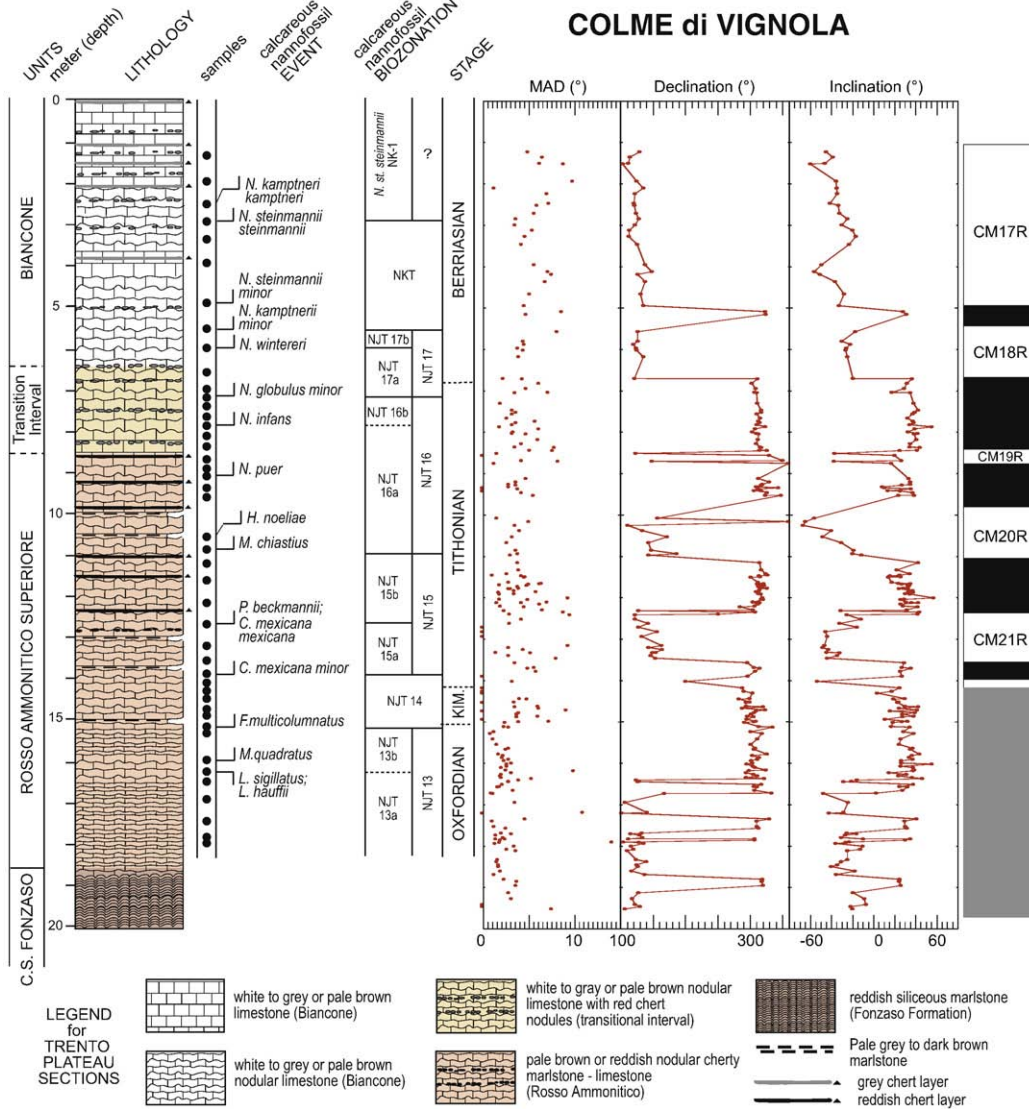


Fig. 5. The lithostratigraphy, biostratigraphy and magnetostratigraphy of the Colme di Vignola section. Component declination and inclination, with maximum angular deviation (MAD) values, are interpreted in terms of normal (black blocks) and reverse (white blocks) polarity zones.

been extended into the lowermost Cretaceous. In Fig. 11, we summarize the biostratigraphic framework, as adopted for the Callovian–Berriasi-an interval, and its integration into the geomagnetic polarity timescale (GPTS) of Channell et al. (1995a) for the Berriasi-an–Kimmeridgian interval and the timescale of Ogg et al. (2008) for the Oxfordian–Callovian interval. Although further investigations are required to better constrain ages of nannofossil events in the Callovian–Kimmeridgian interval, Upper Jurassic stage boundaries can be correlated as follows: the last occurrence (LO) of *C. wiedmannii* correlates with the Callovian/Oxfordian boundary (Mattioli and Erba, 1999), the first occurrence (FO) of *F. multicolumnatus* is a latest Oxfordian event (De Kaenel et al., 1996; Ogg et al., 2008), the FOs of *N. steinmannii minor* and *N. kamptneri minor* are close to the Tithonian/Berriasi-an (J/K) boundary (Wimbledon, 2009; Wimbledon, submitted for publication). The appearance of primitive nannoconids (FOs of *N. infans* and *N. puer*) is dated as earliest late Tithonian (Casellato, submitted for publication). The Kimmeridgian/Tithonian boundary cannot be identified precisely by nannofossil events, although it is bracketed by the FOs of *Z. fluxus* and *Z. embergeri* (Casellato, submitted for publication). Both taxa are extremely rare in the sections from the Trento Plateau area and consequently the identification of the Kimmeridgian/Tithonian boundary remains problematic.

Our biostratigraphic study was based on smear slides made from samples with an average stratigraphic spacing of 20–50 cm, with the exception of Frisoni B that was studied every meter. All smear slides were prepared from the drill-cores used for paleomagnetism. A small amount of rock material was powdered and mixed with a few drops of double-distilled water. The obtained suspension was mounted on a microscope slide, covered with a slide cover and fixed with Norland Optical Adhesive, without centrifuging, ultrasonic cleaning or settling of sediment in order to retain the initial composition. In the case of Torre de' Busi, nannofossil investigations were also conducted on thin sections, prepared from the same core pieces used for smear slides. Nannofossil assemblages were analyzed with a polarizing light microscope, at 1250 \times magnification.

Calcareous nannofloral preservation is poor to moderate, and abundance is rare to common. In particular, nannofossils are rare to few in the lower interval (Radiolariti, lower Rosso ad Aptici and Rosso Ammonitico), and become few to common in the upper interval (upper Rosso ad Aptici, Rosso Ammonitico Superiore and Maiolica/Biancone). Assemblages are dominated by the genus *Wattnaueria* in the Radiolariti, lower Rosso ad Aptici and Rosso Ammonitico intervals, then genera *Conusphaera* and *Polycostella* become common to abundant in the upper Rosso ad Aptici-transition to Maiolica and

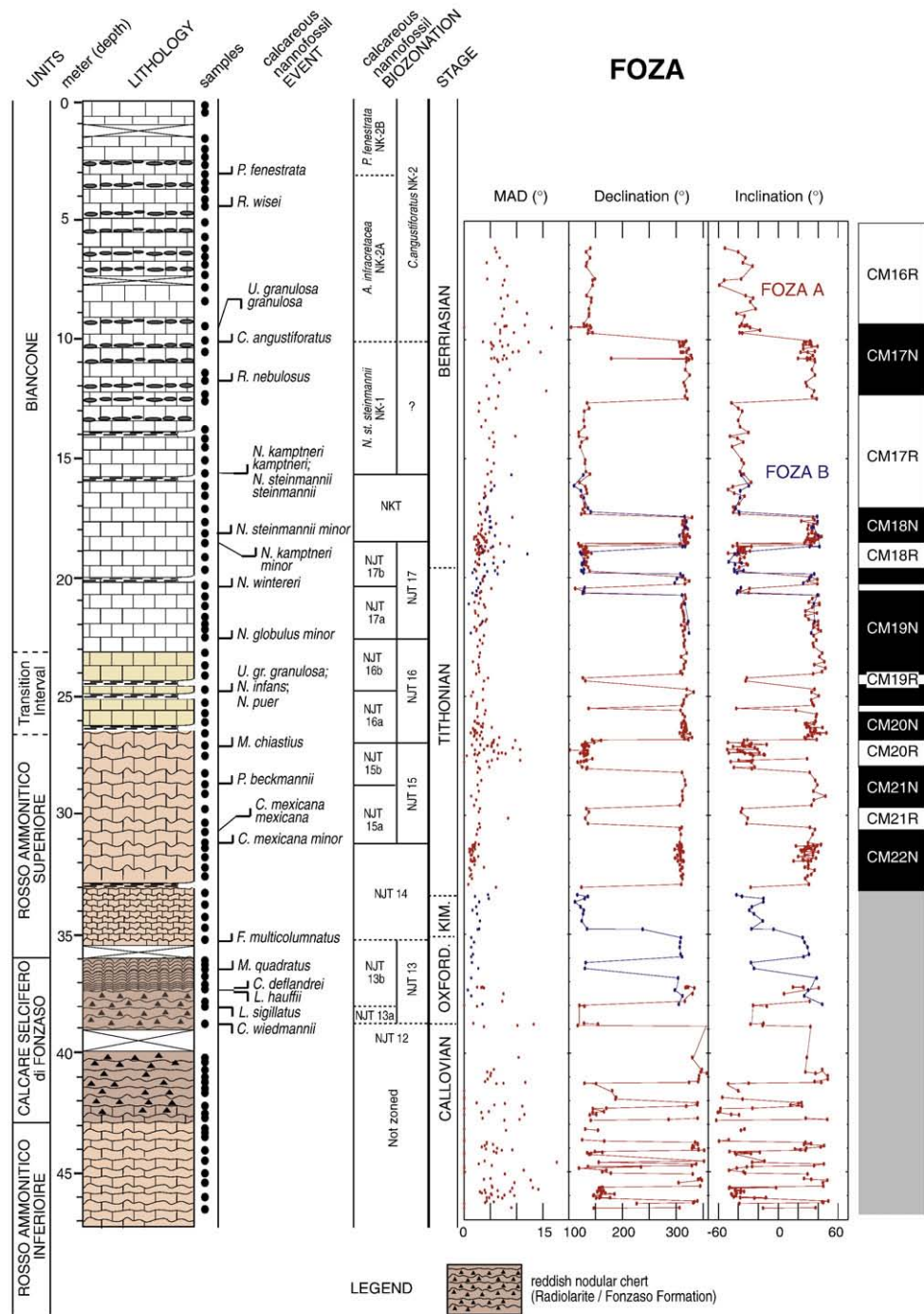


Fig. 6. The lithostratigraphy, biostratigraphy and magnetostratigraphy of the Foza sections. Paleomagnetic data in red and blue were derived from Foza A and Foza B, respectively (see text). Although the correlation to Foza B (in blue) to the upper interval from Foza A seems secure, the lower interval from Foza B cannot be adequately correlated to Foza A. Component declination and inclination, with maximum angular deviation (MAD) values, are interpreted in terms of normal (black blocks) and reverse (white blocks) polarity zones.

upper Rosso Ammonitico Superiore-transition to Biancone. In the Maiolica/Biancone limestones, nannofossil assemblages are characterized by high abundance of the genus *Nannoconus*. Most of the expected Late Jurassic and earliest Cretaceous nannofossil events were detected, allowing the identification of the zones and subzones reported in Fig. 11.

At Torre de' Busi, all Oxfordian-Tithonian events, zones and subzones have been recognized (Fig. 3). The uppermost Radiolarite can be assigned to the Kimmeridgian, because the lithostratigraphic boundary is definitely younger than the latest Oxfordian FO of *F. multicolumnatus*. A number of Tithonian events have been detected in

the upper Rosso ad Aptici through Maiolica formations. The lower Rosso ad Aptici is dated as middle early Tithonian, based on the FOs of *C. mexicana minor*, *C. mexicana mexicana* and *P. beckmannii*. The FO of *N. infans* provides an early/late Tithonian age for the beginning of the Rosso ad Aptici-Maiolica transition interval. In the lowermost part of Maiolica, the FOs of *N. steinmannii minor* and *N. kampfneri minor* are markers for the Tithonian/Berriasian (J/K) boundary.

The Colle di Sogno section was studied in the Calcare di Moltrasio-Calcare di Domaro-Sogno Formation interval (Fig. 4). Calcareous nannofossils are rare (Calcare di Moltrasio) to common (Sogno Formation) and poorly to moderately preserved. Most of the late

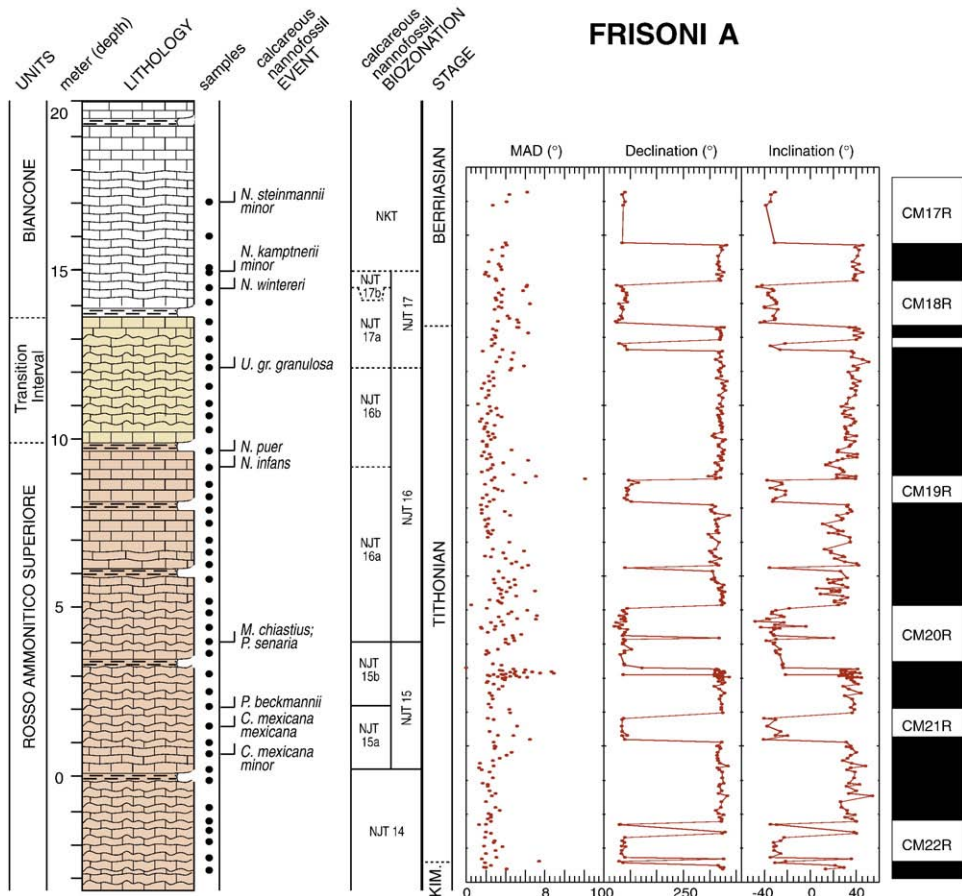


Fig. 7. The lithostratigraphy, biostratigraphy and magnetostratigraphy of the Frisoni A section. Component declination and inclination, with maximum angular deviation (MAD) values, are interpreted in terms of normal (black blocks) and reverse (white blocks) polarity zones.

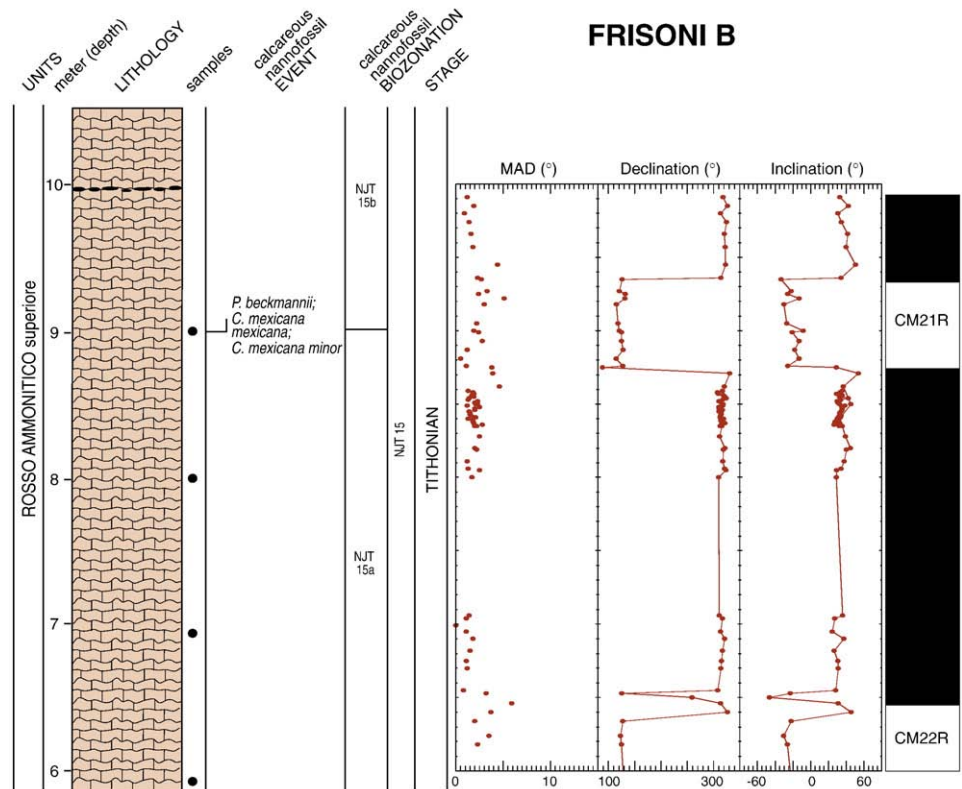


Fig. 8. The lithostratigraphy, biostratigraphy and magnetostratigraphy of the Frisoni B section. Component declination and inclination, with maximum angular deviation (MAD) values, are interpreted in terms of normal (black blocks) and reverse (white blocks) polarity zones.

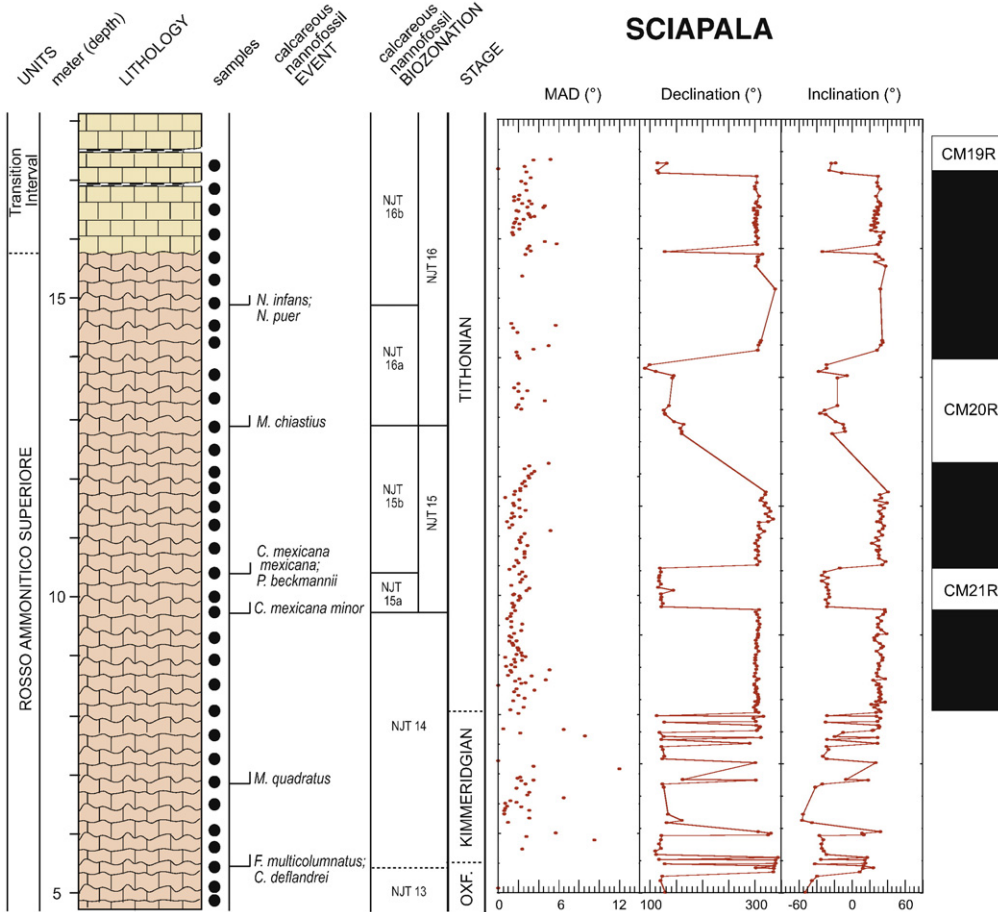


Fig. 9. The lithostratigraphy, biostratigraphy and magnetostratigraphy of the Sciapala section. Component declination and inclination, with maximum angular deviation (MAD) values, are interpreted in terms of normal (black blocks) and reverse (white blocks) polarity zones.

Pliensbachian–earliest Bajocian events (Mattioli and Erba, 1999) were recognized allowing the identification of nannofossil zones NJT 4b through NJT 9 (Fig. 4).

At the Breggia section (near Chiasso, southern Switzerland at 45° 51' N, 9° 00' E), the ammonite biozone stratigraphy of Wiedenmayer (1980) has been correlated to the calcareous nannofossil biostratigraphy of Cobianchi (1992) and magnetostratigraphy of Horner and Heller (1983). The nannofossil and magnetic stratigraphies can be used to correlate the Colle di Sogno and Breggia sections for the Toarcian–Aalenian interval (Fig. 4), consistent with the correlation of lower Toarcian nannofossil events to ammonite finds at Colle di Sogno (Gaetani and Poliani, 1978). The Calcare di Moltrasio–Calcare di Domaro transition is assigned to the lower Pliensbachian; the base of the Sogno Formation correlates with the basal Toarcian, and the base of the Radiolariti is assigned to the lowermost Bajocian. In the lower part of the Sogno Formation, the so-called “Fish Level” is the local manifestation of the Toarcian Oceanic Anoxic Event (T-OAE). No black shales occur in the lower part of the Rosso Ammonitico Lombardo at Breggia, where there appears to be a hiatus at the *Tenuicostatum–Serpentinus* zonal boundary.

Calcareous nannofossil results for the Trento Plateau sections confirm the highly condensed and discontinuous nature of the Rosso Ammonitico and Calcare Selcifero di Fonzaso, characterized by hiatuses and paraconformities (Ogg, 1981; Martire et al., 2006). Foza (Fig. 6) and Bombatierle (Fig. 10) are the longest sections that have been studied on the Trento Plateau, covering the Rosso Ammonitico Inferiore to Biancone interval. Calcareous nannofossils are rare in the Calcare Selcifero di Fonzaso, rare to few and dominated

by the genus *Watznaueria* in the Rosso Ammonitico Superiore, and common to abundant in the Rosso Ammonitico Superiore–Biancone transition and lower Biancone intervals. Age assignments are based on events in the latest Callovian (LO of *C. wiedmannii*), the latest Oxfordian (FO of *F. multicolumnatus*), the early Tithonian (FO of *C. mexicana minor*) and late early Tithonian (FO *M. chiastius*). The lower/upper Tithonian boundary is marked by the appearance of primitive nannoconids (FOs of *N. infans* and *N. puer*). The upper part of Foza A covers the J/K boundary interval characterized by FOs of *N. steinmannii minor* and *N. kampfneri minor*. The lower/upper Berriasian boundary is placed close to the FO of *C. angustiforatus* (Bralower et al., 1989; Channell et al., 1995a).

At both Foza and Bombatierle, calcareous nannofossils are extremely rare and non-diagnostic in the Rosso Ammonitico Inferiore, therefore no zonal or age assignments could be made (Figs. 6 and 10). The Calcare Selcifero di Fonzaso and lower part of the Rosso Ammonitico Superiore consist of siliceous limestones and extremely condensed nodular limestones, respectively. Two intervals at Foza A (35.4–36.0 m, 39.0–40.0 m) are covered by vegetation and, therefore, were not sampled. Nannofossil events indicate that the Oxfordian–Kimmeridgian interval is severely condensed and possibly partially discontinuous.

Calcareous nannofossils at the Colme di Vignola (Fig. 5), Frisoni A (Fig. 7) and Sciapala (Fig. 9) sections cover the Rosso Ammonitico Superiore to Biancone interval. Calcareous nannofossils are few to rare, poorly preserved and most of the important species have discontinuous ranges. Nevertheless, it was possible to recognize the same succession of marker events described at Foza and Bombatierle and,

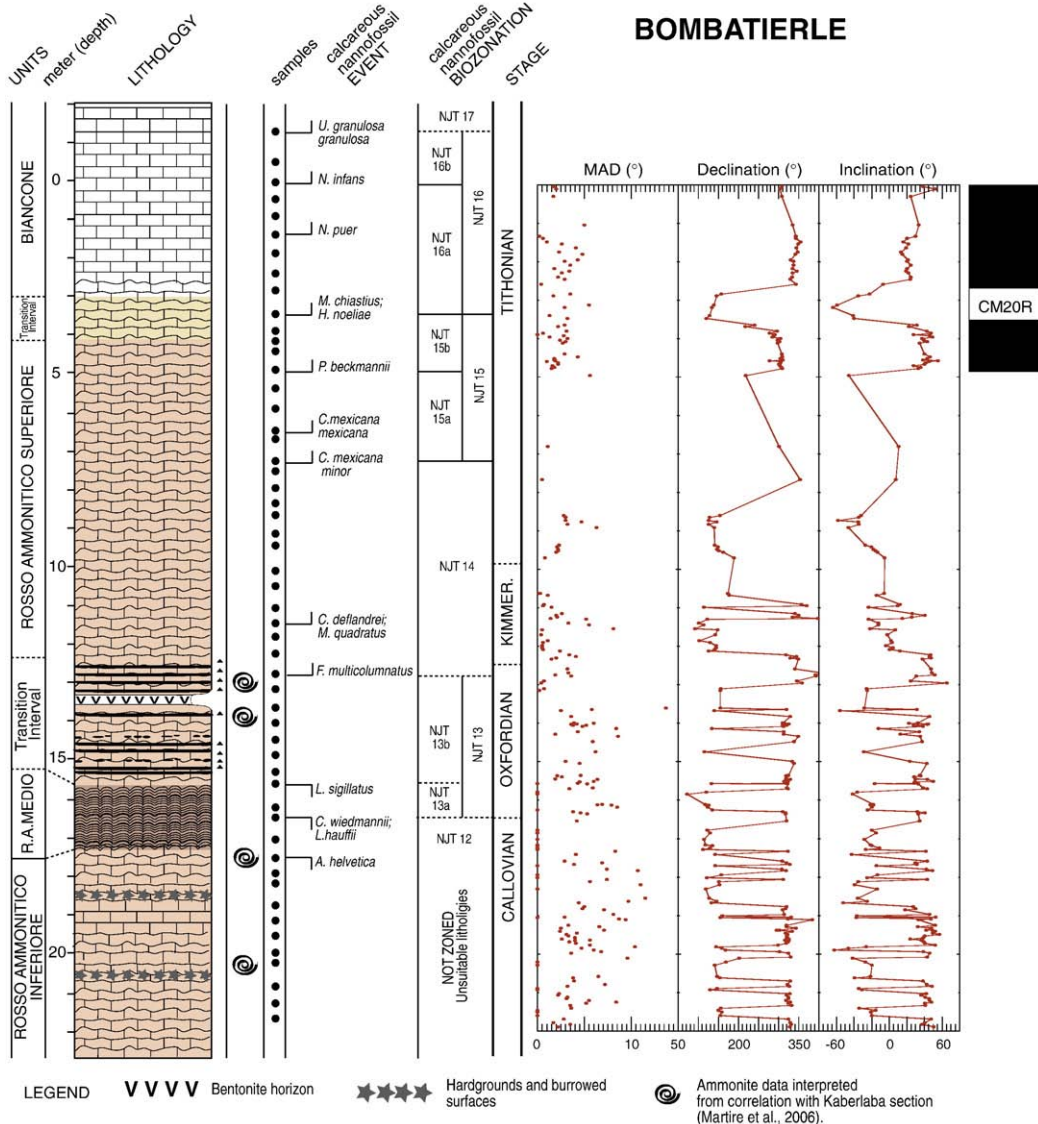


Fig. 10. The lithostratigraphy, biostratigraphy and magnetostratigraphy of the Bombatierle section. Component declination and inclination, with maximum angular deviation (MAD) values, are interpreted in terms of normal (black blocks) and reverse (white blocks) polarity zones.

accordingly, to make stage assignments. The lower Rosso Ammonitico Superiore is late Oxfordian in age based on the LOs of *L. sigillatus* and *L. hauffii*, and FOs of *M. quadratus* and *F. multicolumnatus*. The middle Rosso Ammonitico Superiore is middle early Tithonian in age (FO of *C. mexicana minor*). The beginning of the Rosso Ammonitico Superiore–Biancone transition interval correlates with the lower/upper Tithonian boundary based on the FOs of *N. infans* and *N. puer*. At Colme di Vignola and Frisoni A, the FOs of *N. steinmannii minor* and *N. kampfneri minor* are markers in the lower Biancone limestones.

Frisoni B (Fig. 8) was investigated for calcareous nannofossils in only four samples to derive a zonal-age assignment for correlation with Frisoni A. Nannofossils are few, poorly preserved, and dominated by the genus *Watznaueria*. The FO of *C. mexicana minor* allows the identification of the lower Tithonian (Fig. 8).

The investigated sections from the Trento Plateau area provide nannofossil-derived age assignment of lithostratigraphic units as follows: the Calcare Selcifero di Fonzaso–Rosso Ammonitico Medio are late Callovian–late Oxfordian in age; the Rosso Ammonitico Superiore spans the latest Oxfordian to the early/late Tithonian interval; the transition from the Rosso Ammonitico Superiore to

Biancone is early late Tithonian in age. Ages of lithostratigraphic boundaries are consistent with the chronostratigraphic synthesis of Martire et al. (2006).

The Passo del Branchetto samples yielded rare and poorly preserved nannofossil assemblages dominated by the genus *Watznaueria* that is not diagnostic for age assignment. The only useful event for biostratigraphy in this section is the FO of *F. multicolumnatus* at 3.80 m from the top of the 5.5 m section. This event indicates that the middle part of the sampled section can be assigned to the latest Oxfordian.

A taxonomic index of the calcareous nannofossil taxa, reported here, is included as an [Appendix](#).

4. Paleomagnetism and magnetostratigraphy

Samples for paleomagnetic and biostratigraphic analyses were collected using a hand-held gasoline-powered drill. The stratigraphic spacing of the 2.5-cm diameter drill-cores was generally 10–30 cm. Data gaps in Figs. 3–10 are a result of poorly resolved high unblocking temperature components, and poor exposure in the case of Frisoni B.

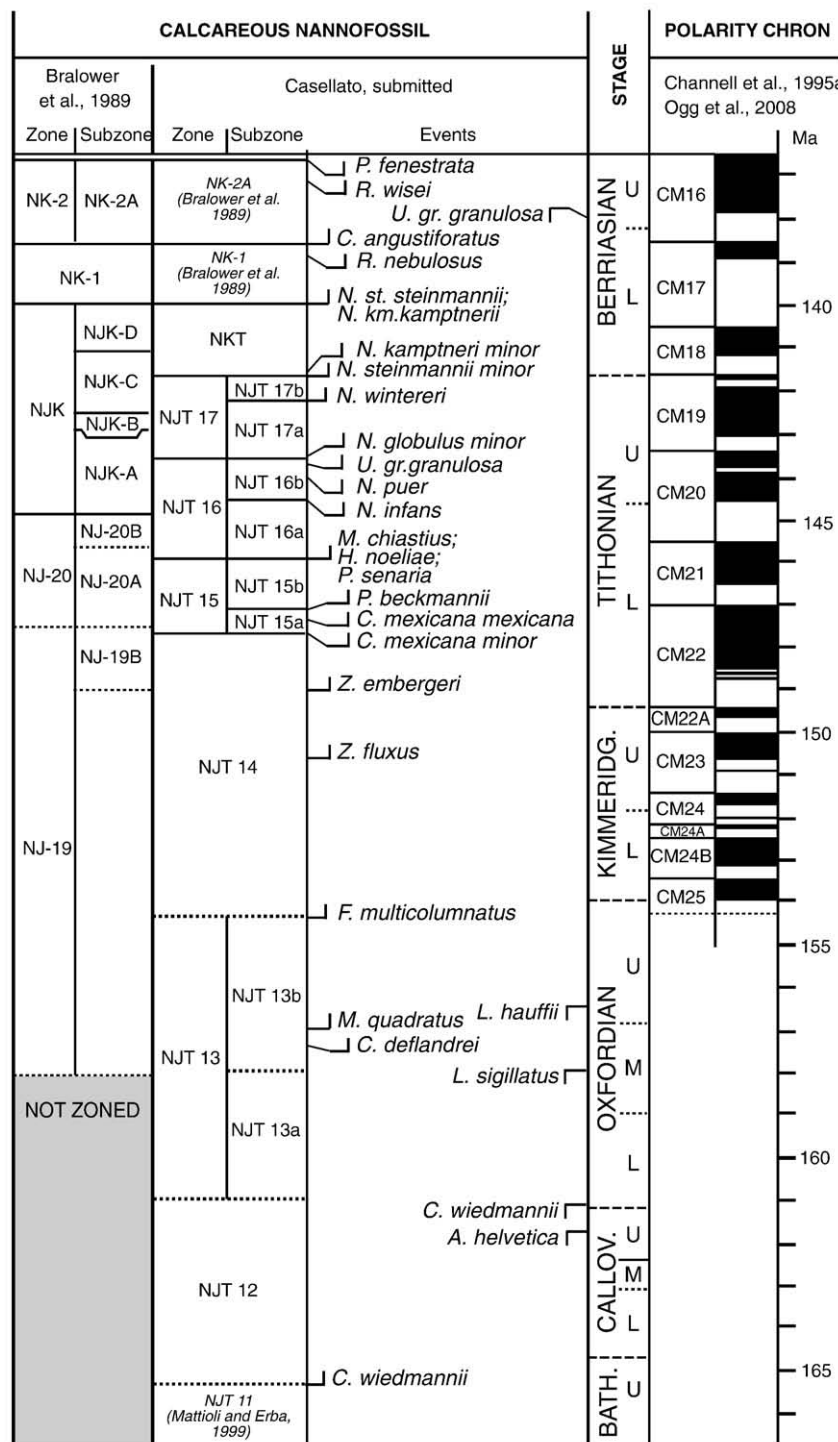


Fig. 11. Synthesis of the biostratigraphic framework (Casellato, submitted for publication) adopted in this paper for the Callovian–Berriasian interval integrated into the geomagnetic polarity timescale (GPTS) of Channell et al. (1995a) for the Kimmeridgian–Berriasian interval and the timescale of Ogg et al. (2008) for the Callovian–Oxfordian interval.

At Torre de' Busi, Foza A, and Frisoni, sample clusters were collected from particular horizons to increase the population of samples for determination of paleomagnetic pole positions. Samples were oriented using a magnetic compass with complementary sun-compass measurements for samples collected close to metallic obstructions (e.g. a metal drainage pipe at Frisoni A). Bedding orientations were measured throughout the sections, using a

magnetic compass and inclinometer, and are used to make bedding tilt corrections to the natural remanent magnetization (NRM) directions.

The NRM of all samples were thermally demagnetized at 25 °C or 50 °C increments in the 100–600 °C temperature range or until the NRM intensity fell below magnetometer noise level, or the NRM became erratic in direction and intensity. Component magnetizations were

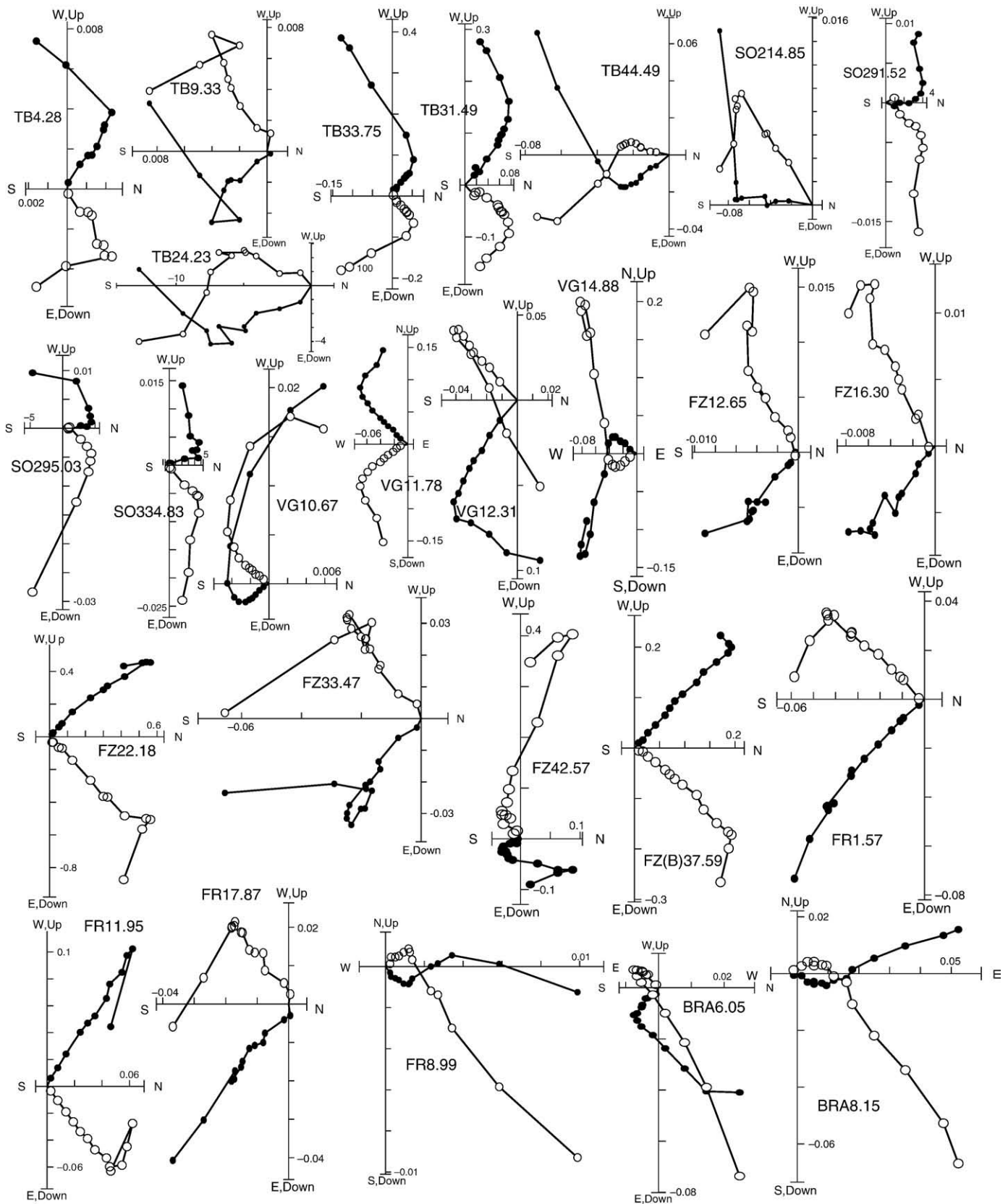


Fig. 12. Orthogonal projections of thermal demagnetization data from Torre de' Busi (TB) in the 20–570 °C interval, Colle di Sogno (SO) in the 20–500 °C interval, Colme di Vignola (VG) in the 20–525 °C interval, Foza A (FZ) and Foza B (FZB) in the 20–560 °C interval, Frisoni A (FR) in the 20–560 °C interval, and Passo del Branchetto (BRA) in the 20–550 °C interval. Closed (open) symbols represent projections on the horizontal (vertical) planes, respectively. Labels indicate meter levels for samples as in Figs. 3–7. Magnetization intensity scales: $\times 10^{-2}$ A/m.

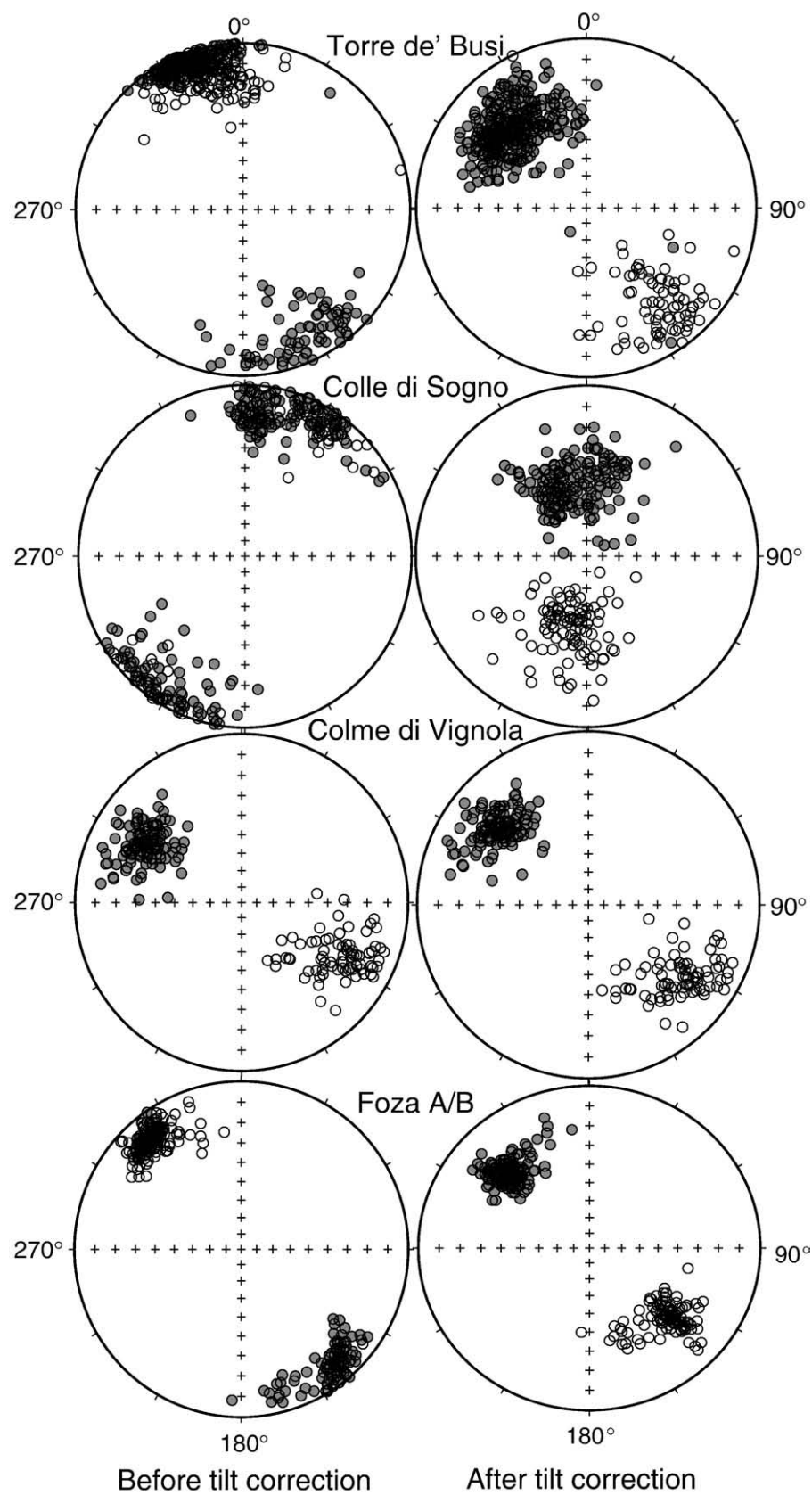


Fig. 13. Equal area stereographic projections before (left) and after (right) bedding tilt correction of component magnetization directions from Torre de' Busi, Colle di Sogno, Colme di Vignola and Foza A and B. Closed (open) symbols represent positive (negative) inclinations.

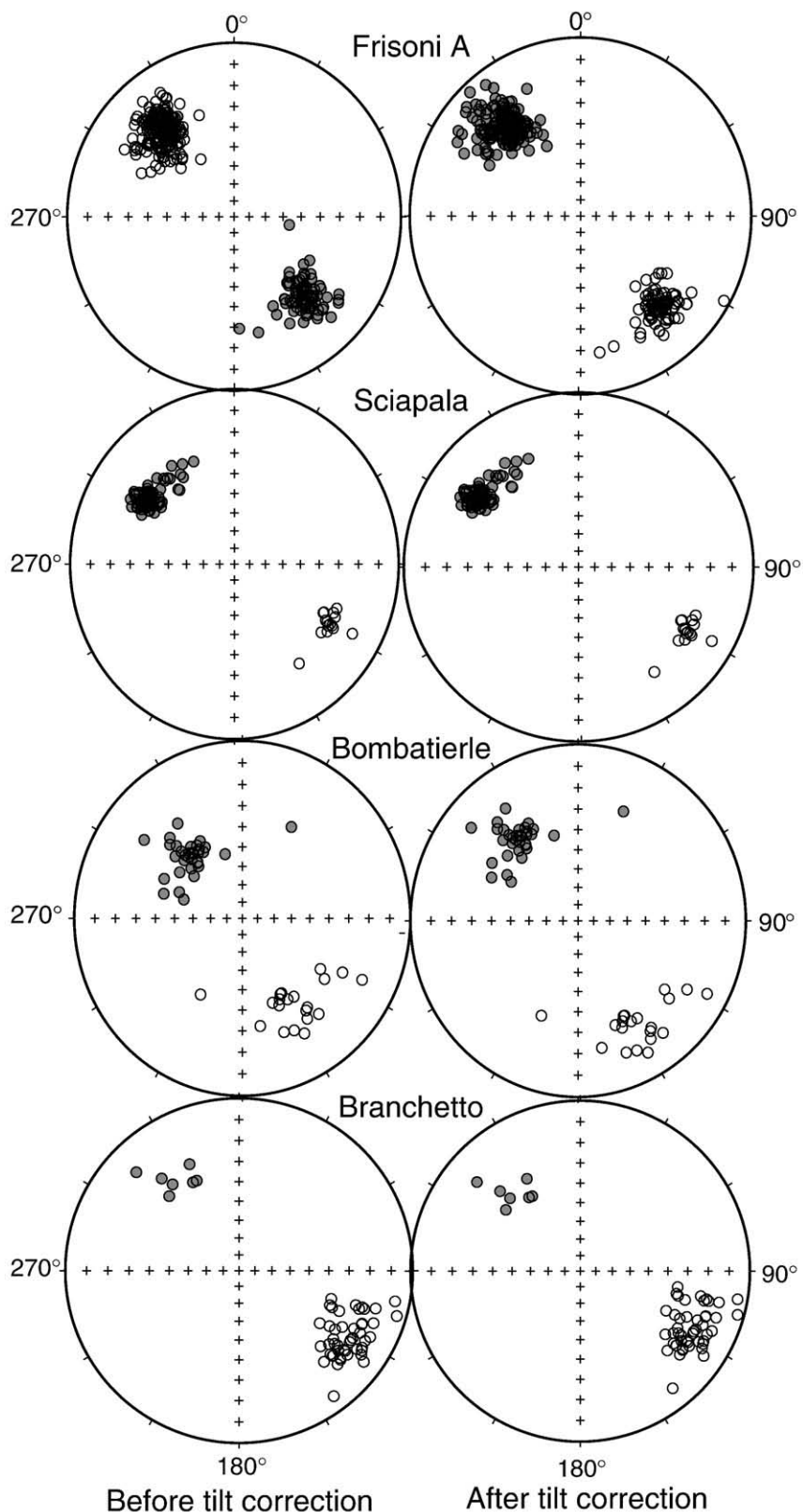


Fig. 14. Equal area stereographic projections before (left) and after (right) bedding tilt correction of component magnetization directions from Frisoni A, Sciapala, Bombatierle, and Passo del Branchetto. Closed (open) symbols represent positive (negative) inclinations.

determined using the standard least squares method (Kirschvink, 1980) applied to a particular demagnetization interval, typically 200–575 °C or temperature limits in this range. Maximum angular deviation (MAD)

values are used to gauge the uncertainty in NRM component directions. Where the MAD values equal to zero in Figs. 3–10, the NRM component cannot be defined other than by picking a stable end-point, due to an

Table 1

Component mean magnetization directions. N: number of samples contributing to the mean direction, GDEC, GINC, BDEC, BINC: declination and inclination in geographic and tilt-corrected coordinates, respectively. PLAT, PLONG: paleomagnetic pole latitude and longitude in tilt-corrected coordinates. RDEC: tilt-corrected component declination after compensation for 10° clockwise rotation of Torre de' Busi and Colle di Sogno (see text). k, α_{95} : Fisher precision parameter and cone of 95% confidence around the mean direction, respectively. K (in Table 2), A_{95} , dp/dm: Fisher precision parameter, cone of 95% confidence around the mean pole, and minor and major axes of ellipse of 95% confidence around the mean pole, respectively. RLAT, RLONG: paleomagnetic pole latitude and longitude in tilt-corrected coordinates, after compensation for 10° clockwise rotation of Torre de' Busi and Colle di Sogno (see text). The paleolatitudes (λ) from Torre de' Busi and Colle di Sogno (Lombardian Basin) are calculated as $\lambda = (90^\circ - \text{colatitude})$ where colatitude is the arc distance from a common site at 45.78°N, 9.48°E (Colle di Sogno) to the individual tilt-corrected paleomagnetic poles. The paleolatitudes (λ) from the Trento Plateau are calculated in the same way with the common site being at 45.69°N, 11.08°E (Passo del Branchetto); paleolatitude error is defined by $\pm A_{95}$. λ_{corr} : corrected mean paleolatitude calculated using the E/I method of Tauxe and Kent (2004) to sites with $N > 80$. Chron/Stage is assigned based on magnetostratigraphy and biostratigraphy. Pole positions in bold are plotted in Fig. 16A.

Location	Chron/Stage	N	G DEC (°E)	G INC (°)	B DEC (°E)	R DEC (°E)	B INC (°)	k	α_{95} (°)	PLAT (°N)	P LONG (°E)	R LAT (°N)	R LONG (°E)	A_{95} (°)	dp (°)	dm (°)	$\lambda(\text{N})$ (entry in Fig. 18)	λ_{corr} (°N)
Torre de' Busi	CM18–19	127	351.5	−14.3	326.0	316.0	43.7	30	2.3	56.2	254.5	49.6	264.8	2.5	1.8	2.9	25.6 (7)	Reject.
	CM20	249	331.2	−8.5	321.7	311.7	29.9	23	1.9	46.4	249.1	40.1	259.2	1.6	1.2	2.1	16.0 (6)	
	CM21n	64	338.9	−8.7	315.3	305.3	33.1	42	2.8	43.9	257.7	37.2	266.6	2.4	1.8	3.1	18.1 (5)	
	CM22n– late Oxf.	63	338.5	−11.4	327.1	317.1	23.5	41	2.8	46.4	239.9	40.6	250.7	2.4	1.6	3.0	12.3 (4)	
Colle di Sogno	Toar.–Aalen.	104	33.6	−5.5	9.7	359.7	52.0	15	3.7	74.9	156.3	76.8	190.5	4.7	3.5	5.1	32.7 (3)	Reject.
	Pliensbach.	83	28.3	−1.4	6.6	356.6	54.5	25	3.1	78.1	162.1	78.9	204.0	3.6	3.0	4.3	35.0 (2)	35.4
	Sinemurian	85	5.5	15.8	335.3	325.3	54.6	45	2.3	68.5	258.3	61.8	269.5	2.7	2.3	3.3	35.1 (1)	36.5
Colme di Vignola	CM17–19	58	299.8	30.8	309.0		34.8	45	2.8	40.5	265.9			2.5	1.9	3.2	19.0 (19)	20.9
	CM20–21	65	306.3	35.4	316.0		32.4	34	3.1	44.1	258.0			2.8	2.0	3.5	17.5 (16)	–
	CM22	87	296.6	30.9	304.5		28.5	38	2.5	34.7	266.2			2.3	1.5	2.7	15.1 (11)	17.0
Foza A	CM17–19	135	321.0	−14.3	314.1		36.3	121	1.1	44.6	262.8			1.0	0.8	1.3	20.3 (20)	22.4
	CM20–21	73	319.2	−14.7	312.9		33.2	63	2.1	42.3	262.0			1.8	1.4	2.4	18.2 (17)	–
	CM22	41	314.2	−15.0	308.2		30.7	134	1.9	38.1	264.7			1.4	1.2	2.2	16.6 (12)	–
	Callovian	23	342.9	−17.4	339.2		38.0	52	4.2	60.1	233.2			3.7	3.0	5.0	21.2 (8)	–
Frisoni A	CM18–19	113	319.6	−30.9	319.4		35.0	88	1.4	47.4	256.7			1.3	0.9	1.6	19.4 (18)	22.7
	CM20–21	122	317.3	−38.2	316.9		30.0	58	1.7	43.4	256.3			2.2	1.0	1.9	16.2 (15)	19.0
	CM22	47	309.1	−38.8	309.2		33.2	96	2.1	39.9	265.4			1.8	1.4	2.4	18.3 (13)	–
Sciapala	CM21–22	97	305.9	35.7	305.8		30.7	108	1.4	36.5	266.9			1.4	0.9	1.5	16.7 (14)	17.2
Bombatierle	Oxf.–Call. ?	53	321.8	47.3	324.6		36.7	25	4.0	51.6	251.9			4.0	2.7	4.6	20.4 (9)	–
P. Branchetto	Late Oxf. (CM25?)	54	304.0	27.7	299.3		28.1	32	3.5	30.9	270.9			3.2	2.1	3.8	15.2 (10)	–

erratic decay of the component magnetization direction into the origin of the orthogonal projection. Typical orthogonal projections of thermal demagnetization data are given in Fig. 12 indicating, in general, that characteristic high blocking temperature magnetization directions are adequately defined during thermal demagnetization, yielding populations of normal and reverse magnetization components before and after bedding tilt correction (Figs. 13 and 14). Low blocking temperature (LBT) overprints are apparent at all sections, particularly at Colle di Sogno and Colme di Vignola (VG), and Passo del Branchetto (BRA) where LBT component are often apparent up to demagnetization temperatures of ~350 °C (Fig. 12). The fairly straightforward NRM characteristics are consistent with numerous previous paleomagnetic studies in the Maiolica and Rosso Ammonitico facies, and in the underlying formations exposed at Colle di Sogno and Torre de' Busi, that

indicate primary magnetizations carried by magnetite, with minor pigmentary hematite contributing to secondary magnetizations in the Rosso Ammonitico facies (e.g. Ogg, 1981; Channell et al., 1987, 1992; Muttoni et al., 2005).

For Torre de' Busi (Fig. 3), Foza (Fig. 6), and Frisoni A (Fig. 7), the component magnetization directions yield a clear pattern of polarity zones that can be unequivocally correlated to the GPTS. Fingerprints in the polarity zone pattern such as the reverse polarity zones within CM19N and CM20N (CM19N-1r and CM20N-1r) are particularly distinctive (Figs. 3, 6 and 7) and have been observed in numerous other magnetostratigraphic sections and in the marine magnetic anomaly record (see Channell et al., 1995a for GPTS in this interval). The polarity pattern resolved from the other sections is less easy to identify, in terms of polarity chronos, either because magnetization

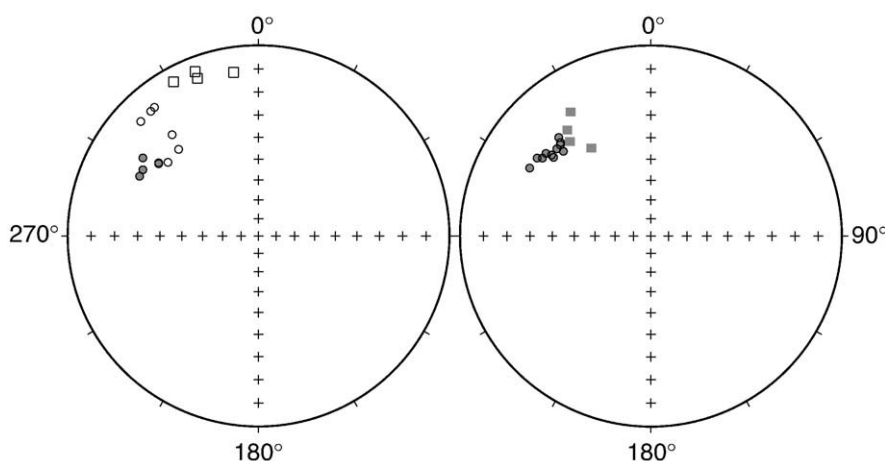


Fig. 15. Equal area stereographic projections before (left) and after (right) bedding tilt correction of component mean magnetization directions for all CM17 to CM23 subdivisions listed in Table 1. Mean directions from Torre de' Busi are shown as square symbols. Closed (open) symbols represent positive (negative) inclinations.

Table 2

Sites with acronym as plotted in Fig. 18. Age (Ma): nominal ages derived from biostratigraphy adopting the time scale of Ogg et al. (2008) for the Rhaetian–Oxfordian, and of Channell et al. (1995a) for the Kimmeridgian–Aptian. Note that Muttoni et al. (2005) adopted for the entire Rhaetian–Aptian time interval the Gradstein et al. (2004) time scale, which is identical to Ogg et al. (2008) for the Rhaetian–Oxfordian but markedly different from Channell et al. (1995a) for the Kimmeridgian–Aptian; errors (\pm Ma) express estimated time span of sites; for magmatic units, ages are radiometric with methods described in listed publications. N: number of characteristic component directions or, when indicated, of paleomagnetic sites or overall means. Paleolatitude (λ) error is defined by $\pm A_{95}$ or it is approximated by $\pm dp$.

Acronym	Site	Age (Ma)	Rock unit	N	In situ coordinates			Tilt-corrected coordinates									Ref.					
					k	α_{95} (°)	GDEC (°E)	GINC (°)	k	α_{95} (°)	BDEC (°E)	BINC (°)	NORM (%)	PLAT (°N)	PLONG (°E)	K	A_{95} (°) dp/dm	λ (°N)	RDEC (°E)	RLAT (°N)	RLONG (°E)	
<i>Southern Alps (Lombardian basin) sediments</i>																						
VC	VALCAVA	199.6 \pm 0.50	Zu Fm. (T/J bound.)	60	14	5.1	9.7	19.7	14	5.1	359.2	54.6	80	80.6	197.3	11	5.9	37 ^a		Muttoni et al. (2005)		
CS1	COLLE SOGNO1	194 \pm 0.15	Moltrasio Fm.	13	96	4.3	12.5	7.4	96	4.3	349.8	49.4	100	72.9	220.4	74	4.8	31 ^a	339.8	67.9	241.7	Muttoni et al. (2005)
CS2	COLLE SOGNO2	189.6 \pm 0.15	Moltrasio Fm.	12	24	9.0	12.3	13.7	23	9.3	330.6	48.5	100	63.0	254.2	18	10.5	30 ^a	320.6	55.3	265.2	Muttoni et al. (2005)
AT	ALPE TURATI	186–183	Domaro Fm.	62	–	–	–	–	–	6.7	337.3	43.2	34	62.5	238.3	–	5.2/8.3	25 ^a		Hornor and Heller (1983)		
CS3	COLLE SOGNO3	184.5 \pm 0.10	Domaro Fm.	11	24	9.5	205.4	0.4	24	9.5	188.8	–47.6	27	73.3	161.9	24	9.5	31 ^a	358.8	72.9	192.9	Muttoni et al. (2005)
CS4	COLLE SOGNO4	183.3 \pm 0.15	Domaro Fm.	13	18	9.9	18.6	4.0	17	10.3	353.4	44.5	54	71.4	202.9	14	11.3	28 ^a	343.4	66.3	229.0	Muttoni et al. (2005)
CS5	COLLE SOGNO5	179.2 \pm 0.15	Sogno Fm.	13	26	8.3	201.9	10.4	26	8.3	184.2	–42.8	0	68.9	178.6	18	10.1	25 ^a	354.2	68.5	203.8	Muttoni et al. (2005)
CS6	COLLE SOGNO6	176 \pm 0.10	Sogno Fm.	9	33	9.1	12.2	3.1	33	9.1	344.7	39.6	78	63.8	222.3	24	10.8	23 ^a	334.7	58.9	239.2	Muttoni et al. (2005)
CS7	COLLE SOGNO7	172 \pm 0.20	Sogno Fm.	10	65	6.0	24.5	–13.9	65	6.0	7.6	44.3	67	69.5	170.0	48	7.0	26 ^a	357.6	70.1	195.7	Muttoni et al. (2005)
CS7B	COLLE SOGNO7B	167.7 \pm 0.10	Green radiolarites	5	No characteristic components isolated														Muttoni et al. (2005)			
CS7C+D	COLLE SOGNO7C+D	165–163	Green radiolarites	3	53	17.1	20.0	–25.2	52	17.2	18.1	29.1	0	56.1	156.8	43	18.9	15 ^a		Muttoni et al. (2005)		
CS8	COLLE SOGNO8	161.8 \pm 0.10	Red radiolarites	12	40	7.0	185.8	2.4	46	6.4	174.4	–18.1	33	53.3	199.0	59	5.7	9 ^a	344.4	51.1	214.3	Muttoni et al. (2005)
CS9	COLLE SOGNO9	151.0 \pm 0.80 ^b	Base Rosso Aptici Fm.	7	68	7.3	172.5	7.9	68	7.4	165.0	–17.7	43	51.2	213.6	157	4.8	9 ^a	335.0	47.5	227.4	Muttoni et al. (2005)
CS10	COLLE SOGNO10	143.5 \pm 0.50 ^c	Top Rosso Aptici Fm.	13	16	10.9	146.7	11.1	23	8.8	135.6	–23.2	46	39.9	252.2	31	7.5	12 ^a	305.6	33.2	261.0	Muttoni et al. (2005)
CS11	COLLE SOGNO11	143.2 \pm 0.25 ^c	Lower Maiolica Fm.	12	101	4.3	344.0	–20.2	100	4.4	329.2	35.8	100	53.9	244.3	103	4.3	20 ^a	319.2	47.7	255.3	Muttoni et al. (2005)

PU	PUSIANO	136.5–127.3 ^c	Maiolica Fm. M15–M7	185	5	5.1	322.8	–43.3	5	5.4	326.7	47.8	mix	59.0	258.1	–	4.6/7.0	29 ^a	Channell et al. (1993)
PO	POLAVENO	138.5–124 ^c	Maiolica Fm. M16–M3	504	–	–	332.8	19.0	21	1.4	319.3	36.7	mix	48.3	256.7	–	0.9/1.6	21 ^a	Channell et al. (1995b)
SG	SAN GIOVANNI	130–124 ^c	Maiolica Fm. M10–M3	86	24	3.2	333.1	21.4	32	2.7	323.4	36.0	56	50.5	251.9	–	1.8/3.1	20 ^a	Channell and Erba (1992)
PD	PIE' DEL DOSSO	123.5–120.5 ^c	Maiolica Fm. M1–M0	38	31	4.3	16.4	75.2	30	4.3	306.1	40.8	74	41.4	271.7	–	3.2/5.2	24 ^a	Channell and Erba (1992)
AL	ALPETTO	123.5–120.5 ^c	Maiolica Fm. M1–M0	37	–	–	320.3	–23.3	28	4.5	310.8	41.9	mix	45.2	267.7	–	3.4/5.6	24 ^a	Channell et al. (1995b)
<i>Northern Apennines sediments</i>																			
TU1	TUSCAN1 ^d	166–160	Cherts s.s.	16	13	10.8	279.8	21.5	13	10.8	282.2	18.8	62	16.0	279.2	17	9.1	10 ^e	Aiello and Hagstrum (2001)
TU2	TUSCAN2 ^d	156–142 ^c	Siliceous Marls	17	7	14.8	282.6	18.3	10	11.9	280.1	21.8	76	15.8	282.0	15	9.5	12 ^e	Aiello and Hagstrum (2001)
<i>Africa and North America magmatic rocks</i>																			
FR	SIERRA LEONE	193±3	Freetown Complex	67	–	–	–	–	46	6.2	174.8	–6.9	31	82.9	212.7	–	5.6	39 ^a	Hargraves et al. (1999)
NM	N. MAURITANIA	182±5	Hank Volcanics	–	–	–	–	–	99	4.1	342.0	24.0	–	69.4	232.0	–	2.3/4.4	29 ^a	Sichler et al. (1980)
SM	S. MAURITANIA	182±5	Hodh Volcanics	–	–	–	–	–	46	6.1	342.5	18.5	–	71.4	240.2	–	3.3/6.3	32.5 ^a	Sichler et al. (1980)
SMA	SOUTH AFRICA	145±4	Swartruggens Main Kimb.	6	–	–	–	–	56	–	–	–	–	41.6 ^f	274.7 ^f	–	9.0	26 ^a	Hargraves et al. (1989)
NY	NEW YORK	143±3	Ithaca Kimberlite	7	site means	–	–	–	550	2.6	317.3	58.9	86	35.6 ^f	266.4 ^f	–	3.8	17 ^a	Van Fossen and Kent (1993)
NE	NEW ENGLAND	122±3	White Mts. Plutons	3	plutons	–	–	–	–	–	–	–	25	52.5 ^f	258.1 ^f	–	6.9	24 ^a	Van Fossen and Kent (1992)
G2K	SOUTH AFRICA	121(?)–119	Group 2 Kimberlites	7	kimberlites	–	–	–	–	–	–	–	86	56.9 ^f	265.2 ^f	42	9.4	30 ^a	Hargraves et al. (1989)

See caption of Table 1 for key to other symbols.

^a Paleolatitudes calculated at a common site located at 45.78°N, 9.48°E (Colle di Sogno).

^b Age updated with respect to Muttoni et al. (2005) as consequence of new biostratigraphic data from this study.

^c Age updated with respect to Muttoni et al. (2005) as consequence of different time scale.

^d Paleomagnetic overall mean directions and poles recalculated from Aiello and Hagstrum (2001).

^e Paleolatitudes calculated at a common site located at 44.06°N, 10.29°E (TU1 and TU2 average location).

^f Pole rotated into NW African coordinates using rotation parameters from Klitgord and Schouten (1986).

components could not always be adequately defined, or the sampled intervals are highly condensed, or because the polarity template (GPTS) for the interval in question is not well-defined. At Colle di Vignola (Fig. 5), Sciapala (Fig. 9), and Bombatierle (Fig. 10), the magnetization components are not always adequately defined, due to the presence of secondary magnetization components, hence the polarity pattern is poorly defined. In some instances, polarity zone identifications for these sections are aided by the biostratigraphic data, and the polarity zone designations are generally consistent with bio-magnetostratigraphic correlations among the sampled sections. Magnetostratigraphy in the Rosso Ammonitico Inferiore (and Rosso Ammonitico Medio/Calcare Selcifero di Fonzaso) at Bombatierle (Fig. 10) and at Foza (Fig. 6) indicates numerous polarity zones, reflecting both low sediment accumulation rates in this facies, and frequent polarity reversal in the Bajocian to Oxfordian interval (see Ogg, 2004). The condensed nature of the sedimentation, and the lack of a well-defined polarity template for this time interval, inhibits interpretation of polarity zones in terms of polarity chronos and, therefore, definitive correlations of nannofossil events to polarity chronos.

At Colle di Sogno (Fig. 4), the Toarcian–Aalenian polarity zone pattern can be matched to the polarity zone pattern of similar age from the Breggia section (Horner and Heller, 1983) where ammonite biostratigraphy provides age control (Wiedenmayer, 1980). At Colle di Sogno, the lack of unique correlations of polarity zones to polarity chronos is a consequence of the poorly-constrained Pliensbachian–Aalenian GPTS (e.g. Ogg, 2004) and the relatively low resolution of the biostratigraphy in this interval.

5. Bio-magnetostratigraphy and stage boundaries

Integration of nannofossil biostratigraphy and magnetostratigraphy from the investigated sections results in a revised chronostratigraphy for the Kimmeridgian–Berriasiian interval (Fig. 11) and leads to significant refinement of the GPTS. In particular, the latest Oxfordian FO of *F. multicolumnatus* indicates that the Oxfordian/Kimmeridgian boundary correlates with polarity chron CM25. The Kimmeridgian/Tithonian boundary is bracketed by the FOs of *Z. fluxus* (within CM23N) and *Z. embergeri* (within CM22R), of latest Kimmeridgian and earliest Tithonian ages, respectively. The age assignment of the FO of *Z. embergeri* validates previous chronostratigraphy (Bralower et al., 1989; Ogg et al., 2008); *Z. fluxus* is a newly defined taxon (Casellato, submitted for publication) and further investigations are required to confirm the age of its FO. In the absence of ammonite dating, we advocate the correlation of the base of the Tithonian at the onset of CM22. The early/late Tithonian boundary correlates with the onset of CM20N (Channell et al., 1995a; Gradstein et al., 2004) and is marked by the FO of *N. infans*. The Tithonian/Berriasiian (J/K) boundary has been exhaustively investigated by an *ad hoc* Working Group (Wimbledon, 2009), which will eventually submit a formal proposal for the definition of the base of the Cretaceous. Current consensus is that ammonites alone will not provide consistent and widely applicable correlation horizons. The Berriasiian Working Group has been developing an integrated nannofossil–calpionellid biostratigraphy and magnetostratigraphy of the uppermost Tithonian–lowermost Berriasiian interval in Tethyan and Boreal areas. Potential boundary events include the FOs of *N. steinmannii minor* and *N. kampfneri minor*, the base of calpionellid zone B and the onset of CM18R (Wimbledon et al., submitted for publication). Based on current knowledge, we believe that the most reliable nannofossil event is the FO of *N. steinmannii minor* that correlates with the onset of CM18R. We provisionally place the Tithonian/Berriasiian (J/K) boundary at the onset of CM18R (Fig. 11).

As far as the Callovian–Oxfordian interval is concerned, correlation of Boreal versus Tethyan ammonite biozonations is controversial and versions of the GPTS given by Gradstein et al. (2004) and Ogg et al. (2008) are still ambiguous, particularly due to the poorly documented polarity pattern prior to CM25. A number of Callovian–Oxfordian

nannofossil events have been observed in Tethyan sections with partial correlation to ammonites (De Kaenel et al., 1996). The total range of *C. wiedmannii* extends through the Callovian, therefore its FO and LO provide useful biostratigraphic identification of the Bathonian/Callovian and Callovian/Oxfordian boundaries, respectively (Fig. 11). The FO of *C. wiedmannii* was used to identify the top of nannofossil NJT 11 zone (Mattioli and Erba, 1999). Recently, Casellato (submitted for publication) extended the Hettangian–Bathonian Tethyan nannofossil zonation of Mattioli and Erba (1999) to the Callovian–Tithonian interval. Two biozones have been proposed based on reliable nannofossil events, but their calibration with ammonite biostratigraphy and/or magnetostratigraphy is hampered by the widespread occurrence of highly condensed lithologies. The Callovian–Oxfordian interval in the Southern Alps is typically represented by condensed siliceous sediments (Radiolariti, Calcare Selcifero di Fonzaso) and highly condensed nodular limestones (Rosso Ammonitico) characterized by extremely poorly preserved calcareous fossils and frequent hiatuses. In spite of their formation names, ammonite preservation in the Rosso Ammonitico Superiore and Rosso Ammonitico Inferiore formations is generally too poor to yield ammonite zones.

6. Apparent polar wander path (APWP)

We construct APWPs for each of the sampled sections using the magnetic stratigraphies and biostratigraphies for temporal calibration. A similar approach has been applied to sections in the Umbrian Apennines (central Italy) to define the “hairpin turn” in the APWP in the J/K boundary interval, after compensation for large-scale (26°) counter-clockwise attributed to Umbrian deformation (Satolli et al., 2007). We divide the component directions from each section into directional groups based on the interpretation of polarity zones, where possible, and also on biostratigraphy (Table 1). Mean directions for polarity chron groupings listed in Table 1 are shown in Fig. 15. Mean directions from Torre de' Busi (square symbols in Fig. 15) are more northerly, rotated clockwise by $\sim 10^\circ$, relative to the mean directions from the other sections. The “fold test” for these mean directions is positive with precision (k) increasing from 7 to 100 on tilt correction for these 15 mean directions. As the Trento Plateau is located nearer the Adria continental interior (centered in the Adriatic Sea) relative to the Lombardian Basin, we expect the Trento Plateau to be less rotated than the Lombardian Basin relative to Adria–Africa. We therefore apply a 10° vertical-axis rotation “correction” to the Torre de' Busi–Colle di Sogno poles determined here, and to the poles from the same sections determined by Muttoni et al. (2005). The pole positions for each time interval listed in Table 1, together with the Muttoni et al. (2005) data from Table 2, after 10° counter-clockwise rotation of the Torre de' Busi–Colle di Sogno poles, are plotted in Fig. 16A. For Sciapala and Bombatierle (Figs. 9 and 10), the directions are too highly scattered, or too few in number, to yield useful pole positions, apart from the CM21–CM22 interval at Sciapala, and the poorly-constrained Callovian–Oxfordian (Rosso Ammonitico Inferiore) interval at Bombatierle. At Passo del Branchetto, the section yields high blocking temperature component directions that indicate a normal polarity interval overlying a reverse polarity interval (Fig. 14). From the nannofossil biostratigraphy of the Passo del Branchetto section, the sampled section is correlated to the latest Oxfordian in the vicinity of CM25. This site yields the pole position (30°N , 270°E) at the lowest latitude determined in this study and appears to define the cusp in the APWP (Fig. 16A).

Comparison of the pole positions from the Southern Alps with the synthetic APWP for southern Africa (Besse and Courtillot, 2002) (Fig. 16B) indicates that the synthetic African APWP does not fully define the cusp (at 30°N , 270°E) apparent in the new Adria APWP (Fig. 16A). The synthetic Jurassic African APWP of Besse and Courtillot (2002) (Fig. 16B) is located from $>60^\circ\text{N}$ to $\sim 40^\circ\text{N}$ for Early Jurassic to the J/K boundary time (~ 145 Ma) then tracks back to $>60^\circ\text{N}$ by Late

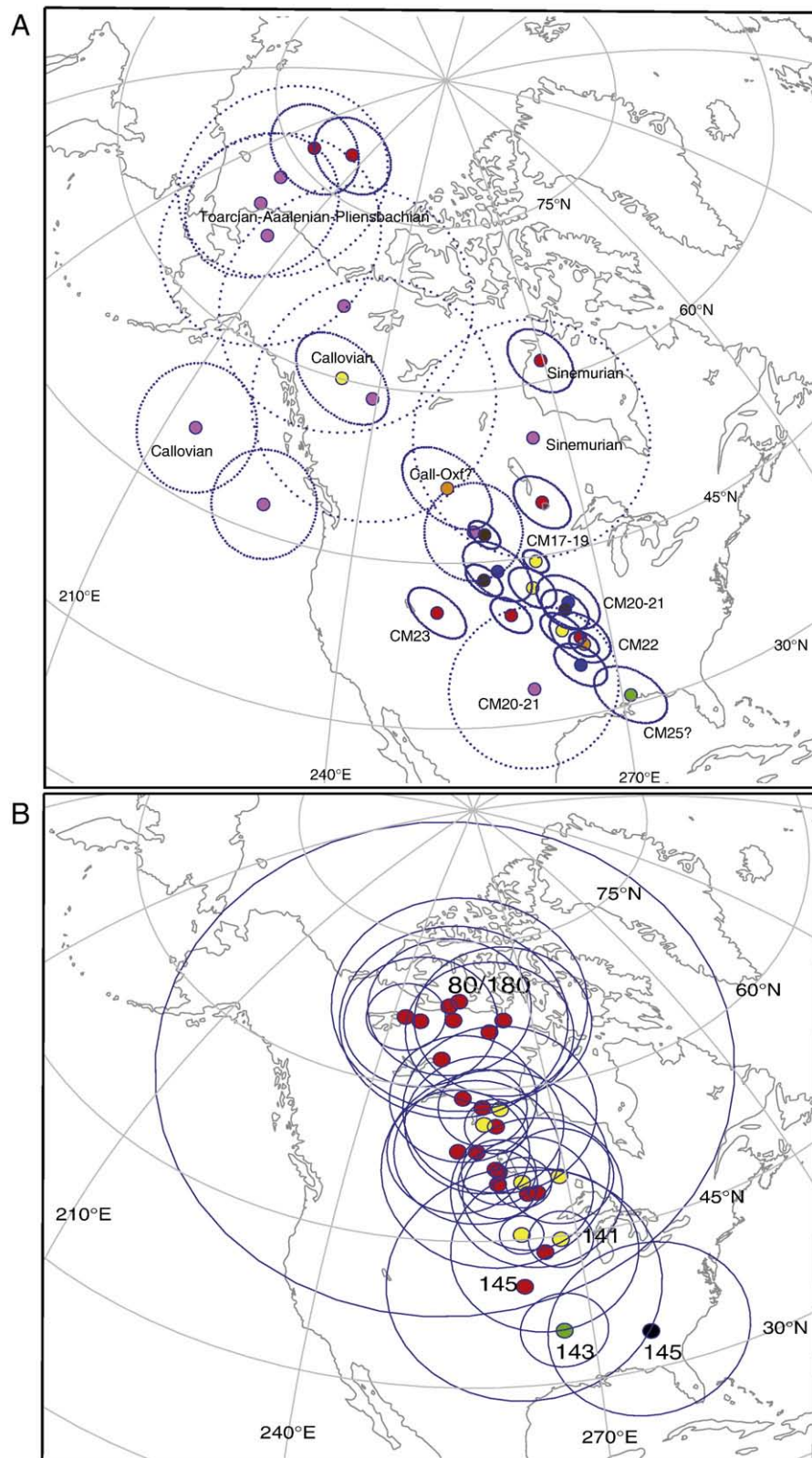
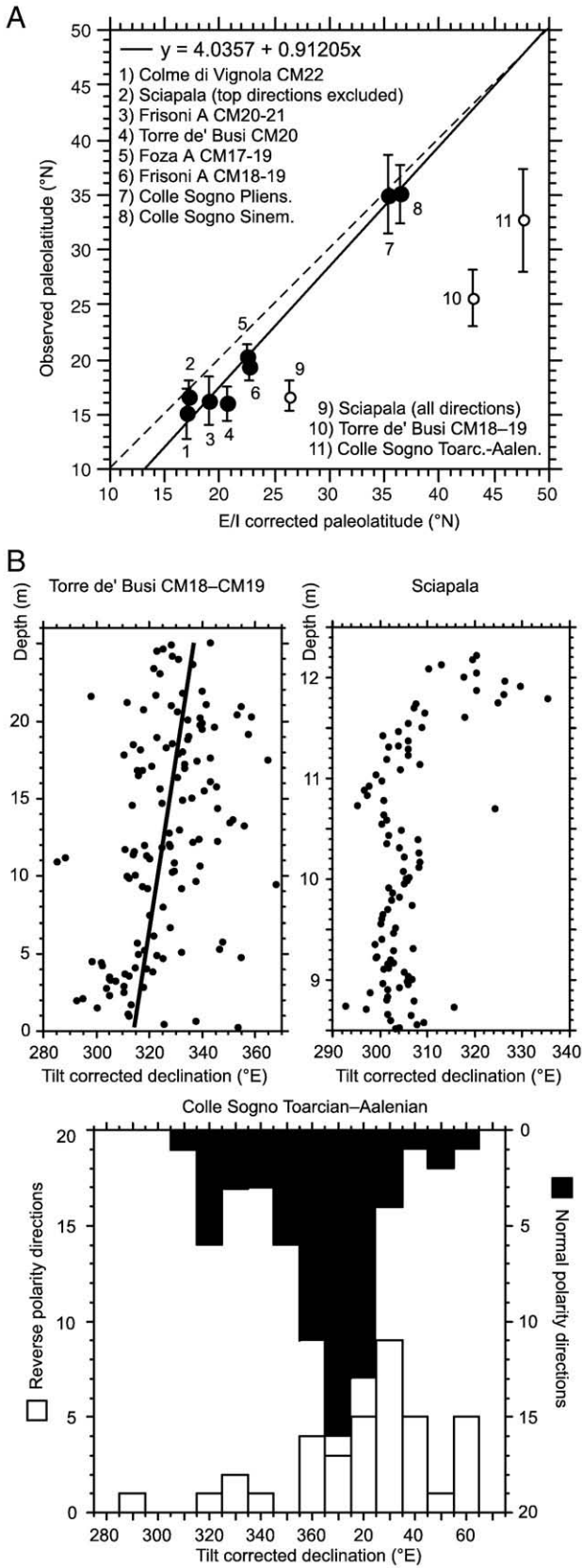


Fig. 16. (A) Apparent polar wander paths (APWP) and poles (from Table 1) for: Torre de' Busi and Colle di Sogno with declinations (RDEC in Table 1) rotated 10° counter-clockwise (red), Colme di Vignola (blue), Foza (yellow), Frisoni (brown), Sciapala and Bombatierle (orange), and Passo del Branchetto (green). Blue circles (ellipses) represent A_{95} (dp/dm) for each pole. (B) Besse and Courtillot (2002) southern Africa synthetic APWP for the 180–80 Ma interval (yellow) with the lowest latitude pole at 145 Ma, the Apennine APWP of Satolli et al. (2007) for the 125–150 Ma interval (yellow) with the lowest latitude pole at 141 Ma, compensated for a 26° vertical-axis counter-clockwise rotation associated with Apennine deformation, compared with poles of appropriate age from Africa (black) (~145 Ma, Hargraves, 1989), and North America (green), rotated to African coordinates (~143 Ma, Van Fossen and Kent, 1993). Blue circles represent A_{95} for each pole.

Cretaceous time (80 Ma). The incomplete definition of the Southern Alpine APWP cusp in the synthetic African APWP is attributed to the lack of data from this time interval for Atlantic-bordering continents,



that define the synthetic APWP of Africa, as well as time interval averaging that is an inevitable part of the APWP construction procedure. The Apennine APWP from Satolli et al. (2007), compensated for a 26° counter-clockwise Apenninic thrust sheet rotation, coincides with the African synthetic APWP but again does not define the cusp in the APWP as observed in the Southern Alps, largely because it is confined to the post-cusp time interval (Fig. 16B).

7. Paleolatitudes

The elongation/inclination (E/I) method of Tauxe and Kent (2004) has been applied to sites with number of directions $N > 80$ (Table 1) to detect possible inclination shallowing associated with sediment deposition and compaction. The E/I corrected paleolatitudes have been found to be only moderately steeper (1–3°) than the non-corrected paleolatitudes (Fig. 17A). In three cases, the E/I method yielded large corrections on the order of 10° or more (Fig. 17A) that are regarded as unrealistic. The Torre de' Busi CM18–19 interval exhibits a clear trend of increasing declination with depth (Fig. 17B) that distorts the overall directional distribution, augmenting scatter in the E-W plane and, as a consequence, it generates an overestimation of corrections from the E/I test. The E/I test applied to data from Sciapala would give a corrected paleolatitude of 26.3°N that is 9.6° higher than the non-corrected paleolatitude; however, the Sciapala declination distribution is clearly skewed in its uppermost part (Fig. 17B). The aberrant declination trends at Torre de' Busi (CM18–19 interval) and Sciapala may be due to unrecognized faulting or to weak and overprinted magnetization components at the top of the two sections. Excluding these uppermost directions at Sciapala would give a corrected paleolatitude of 17.2° that is virtually identical to the original, non-corrected paleolatitude (Table 1). Finally, the Colle di Sogno (Toarcian–Aalenian) site is characterized by strongly non-antipodal directions with the mean normal and reverse directions departing from antipodality by 18°, with the critical angle for a positive reversal test being 7° (Figs. 13 and 17). This site has 41 (out of a total of 104) poorly-defined component magnetization directions with $MAD > 10^\circ$ (Fig. 4). As a result, the overall directional distribution is strongly distorted, thus impeding the execution of a proper E/I test. In conclusion, the E/I method applied to sites with large numbers of samples ($N > 80$) usually yields small paleolatitude corrections of a few degrees. In three distinct cases, however, the E/I method could not be applied because the directional distributions were apparently distorted by factors other than flattening. In some sites, the number of samples was regarded as insufficient for the E/I method. In order to avoid having some sites corrected for inclination shallowing and others not, we adopt the non-corrected poles/paleolatitudes in Figs. 16A and 18, with the caveat that the paleolatitudes may be lower than the 'true' (corrected) paleolatitudes by 1–3°.

The estimates of paleolatitude for Colle di Sogno–Torre de' Busi (Fig. 18, entries 1–7 and Table 1) are integrated with broadly coeval paleolatitudes retrieved by Muttoni et al. (2005) from the same section as well as with paleolatitudes from Jurassic radiolarian cherts

Fig. 17. The elongation/inclination (E/I) method of Tauxe and Kent (2004) has been applied to sites with number of directions $N > 80$ (Table 1) to test for inclination shallowing; the corrected paleolatitudes have been found to be only moderately steeper (1–3°) than the non-corrected paleolatitudes (panel A, black dots). In three cases, indicated by the white dots in panel A and further illustrated in panel B, the E/I method gave large but unrealistic corrections because the directional distributions were distorted by factors other than flattening. Torre de' Busi CM18–19 grouping shows a clear declination/depth trend, whereas Sciapala is characterized by uppermost declinations clearly different from those underlying. These observations may be attributed to unrecognized faulting or to weak and overprinted magnetization components at the top of the two sections. Colle di Sogno (Toarcian–Aalenian) interval is characterized by strongly non-antipodal directions, probably due to incomplete elimination of secondary magnetizations.

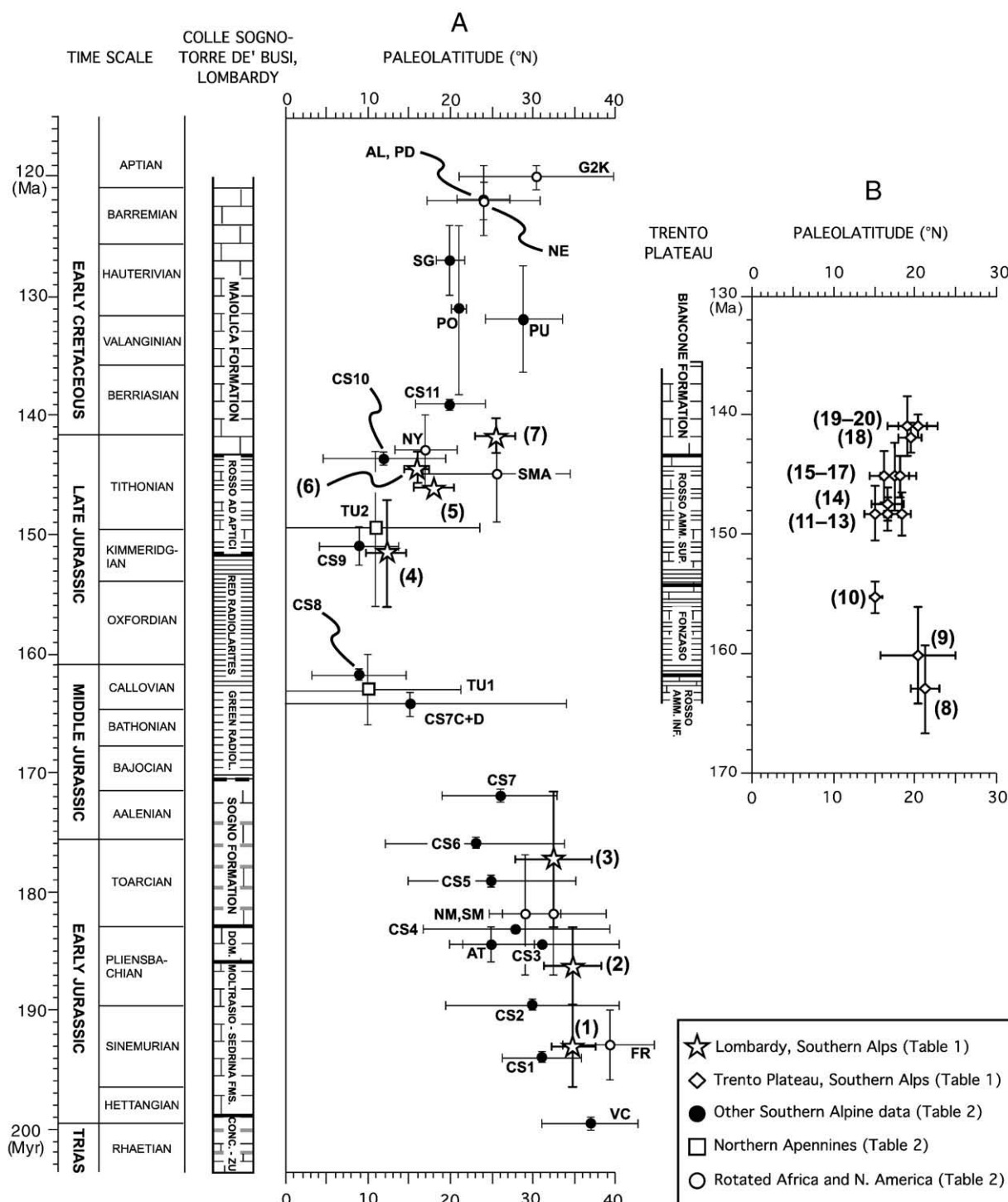


Fig. 18. Paleolatitudinal evolution of the Lombardian Basin based on data from this study (Table 1) and other studies (Table 2) placed alongside the coeval evolution of the adjacent Trento Plateau based on data from this study (Table 1). The time scale adopted is from Ogg et al. (2008) for the Rhaetian–Oxfordian, and Channell et al. (1995a) for the Kimmeridgian–Aptian. For acronyms of paleolatitude entries, see Tables 1 and 2. CONC. = Conchodon Dolomite; ZU = Zu Formation; DOM. = Domaro Formation; RADIOL. = Radiolarites; ROSSO AMM. SUP. = Rosso Ammonitico Superiore; ROSSO AMM. INF. = Rosso Ammonitico Inferiore; FONZASO = Calcare Selcifero di Fonzaso.

of Tuscany (Aiello and Hagstrum, 2001) and from magmatic units from Africa and North America rotated into African coordinates using the rotation parameters of Klitgord and Schouten (1986) (Fig. 18 and Table 2). The resulting composite paleolatitude curve, valid for the Lombardian Basin of Northern Italy, shows a moderate southward drift from 35°N to 25°N in the Early Jurassic followed by values of ~10°N in the Middle–Late Jurassic coincident with Radiolarite–Rosso

ad Aptici deposition. Higher values of 20–30°N appear in the Early Cretaceous during deposition of the Maiolica nannofossil ooze. Paleolatitudes from well-dated magmatic rocks from Africa and North America rotated to northwest Africa coordinates seem to generally confirm this trend (Fig. 18).

Paleolatitudes from the Trento Plateau (Fig. 18, entries 8–20; Table 1) are broadly consistent with coeval paleolatitudes from the

Lombardian Basin, although they show, in general, less variability. It seems that sampling in the condensed Jurassic sequences of the Trento Plateau did not capture the low paleolatitudes observed in the Lombardian Basin during the Callovian–Oxfordian due in part to the sampling gap in the Rosso Ammonitico Medio/Calcare Selcifero di Fonzaso and the lowermost part of the Rosso Ammonitico Superiore.

8. Conclusions

The magneto-biostratigraphies for the Lower Cretaceous from the Maiolica have contributed to correlation of the GPTS to geologic stage boundaries (see [Channell et al., 1995a](#)). The correlation of polarity zones in the Maiolica formation to the GPTS template has been facilitated by several factors that are not present for the earlier Jurassic time: (1) the existence of a marine magnetic anomaly GPTS template, (2) uniform sedimentation rates in the Maiolica limestones leading to a lack of distortion of the polarity zone pattern, and (3) a reliable well-tested biostratigraphy based on nannofossils.

From this study, the correlations of nannofossil events to polarity chron in the Late Jurassic and Jurassic/Cretaceous boundary intervals (**Table 3** and **Fig. 19**) are usually consistent among sections (e.g. FAD of *C. mexicana minor*, *N. steinmannii steinmannii*). Some biostratigraphic horizons are not consistent probably due to low nannofossil abundance and poor preservation. Although the polarity zone pattern is not always unambiguous due to poorly-defined magnetization components, or changes in sedimentation rates that distort the polarity zone pattern, the combined use of polarity stratigraphy and nannofossil biostratigraphy, when tested in multiple sections, provides enhanced stratigraphic control in the Upper Jurassic interval, including the J/K boundary. The J/K boundary can be usefully correlated to, and perhaps defined by, the onset of CM18R, and the Kimmeridgian/Tithonian boundary by the onset of CM22R. These correlations differ with those given by Ogg (2004) and Ogg et al. (2008).

The African APWP for the Jurassic and Cretaceous remains poorly defined, however, the Southern Alpine APWP has been matched to the African APWP based on Jurassic and Cretaceous pole positions mainly from the Venetian Alps (Channell et al., 1992; Channell, 1996), and Permian and Triassic paleomagnetic data (Muttoni et al., 1996, 2003). The Kimmeridgian–Tithonian mean Southern Alpine pole in these

studies has a latitude of 39°N (longitude 263°E), well north of the Kimmeridgian poles resolved here (Table 1, Fig. 16A). The difficulty in defining the cusp in the Southern Alpine APWP (at ~30°N, 270°E) lies with the rapidity of apparent polar wander in this interval and the effect of time averaging on the definition of the cusp. One North American pole dated at 143 Ma from the Ithaca kimberlite, New York (Van Fossen and Kent, 1993), rotated to African coordinates using rotation poles of Klitgord and Schouten (1986), and one pole from the Swartruggens kimberlite of South Africa dated at 145 Ma (Hargraves, 1989), yield poles close to the Southern Alpine cusp (Fig. 16B) implying that the Southern Alpine cusp at ~30°N/270°E is a true feature of the African APWP. The White Mountains of New Hampshire (Van Fossen and Kent, 1990) yield a high latitude pole when rotated to African coordinates (68°N, 270°E). The age of this pole was originally considered to be ~166 Ma, although updated cooling age estimates place it closer to 180 Ma (Eby et al., 1992). The pole lies close to the close to the Early Jurassic (Sinemurian) part of Southern Alpine (Adria) APWP documented here.

The Southern Alpine (Adria) APWP traces a path from $>60^{\circ}\text{N}$ in Early Jurassic time to $\sim 30^{\circ}\text{N}$ at the APWP cusp by latest Oxfordian (Fig. 16A). The biostratigraphically constrained pole position for Pliensbachian to Bajocian from Breggia (Horner and Heller, 1983) supports a higher latitude pole at this time. From analysis of Early Cretaceous paleomagnetic data, the Breggia Gorge has undergone $\sim 25^{\circ}$ clockwise rotation relative to the Southern Alps (Channell et al., 1993). Applying this rotation to the mean direction given by Horner and Heller (1983) yields a Pliensbachian–Bajocian pole (at 74.9°N , 226.3°E) that lies close to the appropriate part of the APWP presented here (Fig. 16A).

The migration of Southern Alpine poles from latitudes $>60^{\circ}\text{N}$ to an apparent cusp close to $30^{\circ}\text{N}/270^{\circ}\text{E}$ appears to have occurred during Bajocian to Oxfordian time (Fig. 16A). During Callovian–Oxfordian time, immediately prior to the APWP arriving at the cusp (at $30^{\circ}\text{N}/270^{\circ}\text{E}$), coincident with the deposition of the Radiolariti in the Lombardian Basin (Fig. 2), the paleolatitude of the region apparently reached values as low as $\sim 10^{\circ}\text{N}$ (Fig. 18). According to the APWP (Fig. 16A) and the paleolatitude evolution (Fig. 18), the \sim Callovian onset of these low Jurassic paleolatitudes for the Southern Alps occurred during the APWP transit from high latitudes to the cusp at $30^{\circ}\text{N}/270^{\circ}\text{E}$, coincident with beginning of oceanic seafloor spreading in the Central Atlantic and Ligurian oceans. Paleolatitudes apparently remained low over the

Table 3

Position of nannofossil events by meter level and within polarity chron, where position in polarity chron is estimated by position in polarity zone, denoted by decimal from base of zone.

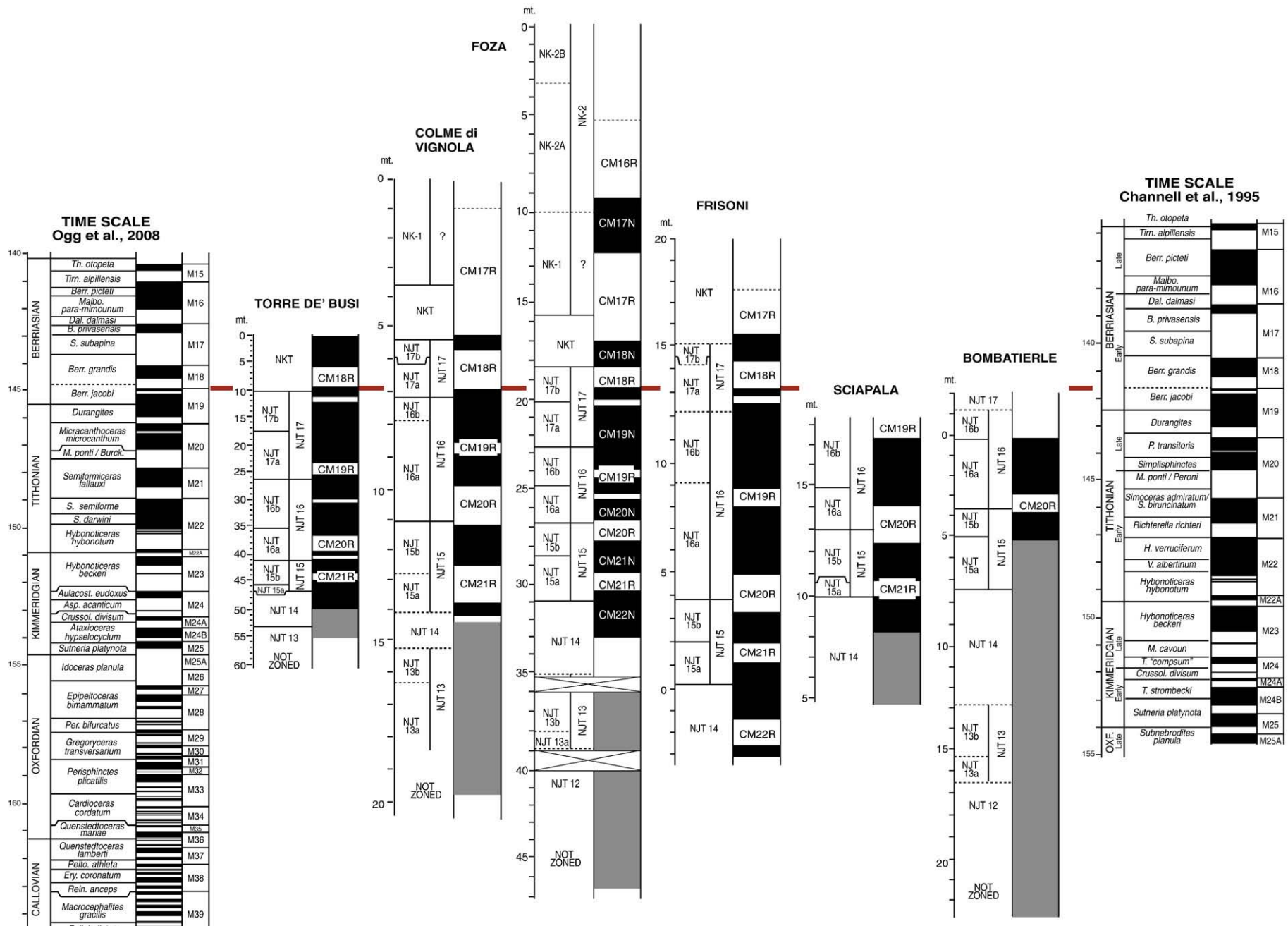


Fig. 19. Synthesis of nannofossil biostratigraphy and magnetostratigraphy in the studied sections with timescales of Ogg et al. (2008) and Channell et al. (1995).

ensuing Oxfordian (for which, however, paleomagnetic data are still largely lacking), and continued to be low during the Kimmeridgian, whereas during Tithonian they became progressively higher, attaining values of 20–30°N by the late Tithonian time (Fig. 18).

The new data test the notion of “pole-by-polarity-chron”, the calibration of an APWP by the use of polarity chron interpretations from magnetostratigraphic sections. The method is useful for cusps in APWPs where poor temporal resolution and time averaging inhibit APWP definition. In the process, we have tested the reliability of nannofossil events by monitoring their match to polarity chronos in multiple Upper Jurassic–lowermost Cretaceous stratigraphic sequences (Table 3 and Fig. 19). These results provide timescale refinements by improving the correlation of the polarity chronos to nannofossil events/zones and hence to geologic stages.

Acknowledgements

Jerry Winterer, Jim Ogg, Eduardo Garzanti and Maurizio Gaetani accompanied one of us (JC) to the Colle di Sogno several decades ago, and initiated our stratigraphic studies of this section. More recently, sampling at the Foza section was aided by Valarian Bachdatsé and his students from the University of Munich. Sampling at quarry sections near Asiago (Sciapala and Bombatierle) was facilitated by officials from the local community. Kainian Huang carried out many of the paleomagnetic measurements with his customary care and attention. Software developed by Chuang Xuan facilitated data analysis. Dennis Kent and Jim Ogg provided valuable reviews of the manuscript. Research supported by the US National Science Foundation through grant EAR-0337102 (JC), and by grant MIUR-PRIN 2007-2007W9B2WE_001 (EE).

Taxonomic appendix

Taxonomic index of calcareous nannofossil taxa reported in this study. Genera, species and subspecies are listed in alphabetic order. Authors and date of the original description and, when necessary, references for subsequent amendments are provided. See Perch-Nielsen (1985), Bralower et al. (1989), Bown and Cooper (1998), Mattioli and Erba (1999) and Casellato (submitted for publication) and references therein for full information regarding taxonomy and references.

- Ansulospaera helvetica* Grün and Zweili, 1980
- Conusphaera mexicana* (Trejo, 1969) subsp. *mexicana* Bralower and Thierstein, in Bralower et al., 1989
- Conusphaera mexicana* (Trejo, 1969) subsp. *minor* Bralower and Thierstein, in Bralower et al., 1989
- Cretarhabdus angustiforatus* (Black, 1971) Bukry, 1973
- Crucilellipsis cuvilliieri* (Manivit, 1956) Thierstein, 1971
- Cyclagelospaera margerelii* Noël, 1965
- Cyclagelospaera deflandrei* Manivit, 1966
- Cyclagelospaera wiedmannii* Reale and Monechi, 1994
- Discorhabdus criotus* Bown, 1987
- Faviconus multicolumnatus* Bralower in Bralower et al., 1989
- Hexolithus noeliae* (Noël, 1956) Loeblich and Tappan, 1963
- Lotharingius hauffii* Grün and Zweili in Grün et al., 1974
- Lotharingius sigillatus* (Stradner, 1961) Prins in Grün et al., 1974
- Microstaurus chiastius* (Worsley, 1971) Bralower et al., 1989
- Microstaurus quadratus* Black, 1971
- Mitolithus lenticularis* Bown, 1987
- Nannoconus globulus* (Brönnimann, 1955) subsp. *minor* Bralower and Thierstein in Bralower et al., 1989
- Nannoconus infans* Bralower in Bralower, Bralower et al., 1989
- Nannoconus kamptneri* (Brönnimann, 1955) subsp. *kamptneri* Bralower and Thierstein in Bralower et al., 1989
- Nannoconus kamptneri* (Brönnimann, 1955) subsp. *minor* Bralower and Thierstein in Bralower et al., 1989
- Nannoconus puer* Casellato, submitted for publication
- Nannoconus steinmannii* (Kamptner, 1931) subsp. *minor* Deres and Achérétéguy, 1980
- Nannoconus steinmannii* (Kamptner, 1931) subsp. *steinmannii* Kamptner, 1931
- Nannoconus wintereri* Bralower and Thierstein in Bralower et al., 1989
- Percivalia fenestrata* (Worsley 1971) Wise, 1983
- Polycopostella beckmannii* Thierstein, 1971
- Polycopostella senaria* Thierstein, 1971
- Rhagodiscus asper* (Stradner, 1963) Manivit, 1971
- Rhagodiscus nebulosus* Bralower and Thierstein in Bralower et al., 1989
- Rucinolithus wisei* Thierstein, 1971
- Umbria granulosa* Bralower and Thierstein in Bralower et al., 1989
- subsp. *granulosa* Bralower and Thierstein in Bralower et al., 1989
- Umbria granulosa* Bralower and Thierstein in Bralower, Monechi and Thierstein, 1989 subsp. *minor* Bralower and Thierstein in Bralower et al., 1989
- Watznaueria britannica* (Stradner 1963) Reinhardt 1964
- Watznaueria contracta* (Bown and Cooper, 1989) Cobianchi, 1992
- Watznaueria fossacincta* (Black 1971) Bown in Bown and Cooper 1989
- Zeugrhabdotus embergeri* (Noël 1958) Bralower et al., 1989
- Zeugrhabdotus fluxus* Casellato, submitted for publication

References

- Aiello, I.W., Hagstrum, J.T., 2001. Paleomagnetism and paleogeography of Jurassic radiolarian cherts from the northern Apennines of Italy. Geological Society of America Bulletin 113, 469–481.
- Barrier, E., Vrielynck, B., 2008. Palaeotectonic maps of the Middle East. Tectono-sedimentary-palinspastic maps from Late Norian to Pliocene. CCGM/CGMW, Paris: 14 maps.
- Baumgartner, P.O., Bernoulli, D., Martire, L., 2001. Mesozoic pelagic facies of the Southern Alps: paleotectonics and paleoceanography. International Association of Sedimentologists, Davos: Field Trip Guide, Excursion A1.
- Bernoulli, D., Jenkyns, H.C., 1974. Alpine, Mediterranean and Atlantic Mesozoic facies in relation to the early evolution of the Tethys. In: Dott Jr, R.H., Shaver, R.H. (Eds.), Modern and Ancient Geosynclinal Sedimentation: SEPM Special Publication, vol. 19, pp. 129–160.
- Bernoulli, D., Jenkyns, H.C., 2009. Ancient oceans and continental margins of the Alpine–Mediterranean Tethys: deciphering clues from Mesozoic pelagic sediments and ophiolites. Sedimentology 56 (1), 149–190.
- Bernoulli, D., Caron, C., Horwood, P., Kalin, O., Stuijvenberg, J.V., 1979. Evolution of continental margin in the Alps. Schweizerische Mineralogische und Petrographische Mitteilungen 59, 165–170.
- Bersezio, R., Erba, E., Gorza, M., Riva, A., 2002. Berriasian–Aptian black shales of the Maiolica formation (Lombardian Basin, Southern Alps, Northern Italy): local to global events. Palaeogeography, Palaeoclimatology, Palaeoecology 180, 253–275.
- Besse, J., Courtillot, V., 2002. Apparent and true polar wander and the geometry of the geomagnetic field over the last 200 Myr. Journal of Geophysical Research 107, B1110.1029/2000JB000050.
- Bosellini, A., 2004. The Western passive margin of Adria and its carbonate platforms. Special Volume of the Italian Geological Society for the IGC 32 Florence, pp. 79–92.
- Bown, P.R., Cooper, M.K.E., 1998. Jurassic. In: Bown, P.R. (Ed.), Calcareous Nannofossil Biostratigraphy. Kluwer Academic, London (UK), pp. 34–85.
- Bralower, T.J., Monechi, S., Thierstein, H.R., 1989. Calcareous nannofossils zonation of the Jurassic–Cretaceous boundary interval and correlation with the geomagnetic polarity timescale. Marine Micropaleontology 14, 153–235.
- Casellato, C.E., 2009. Causes and consequences of calcareous nannoplankton evolution in the Late Jurassic: implications for biogeochronology, biocalcification and ocean chemistry. PhD thesis, Università degli Studi di Milano, Scuola di Dottorato “Terra, Ambiente e Biodiversità”, Dipartimento di Scienza della Terra, Ciclo XXI, 122 pp.
- Casellato, C.E., submitted for publication. Calcareous nannofossil biostratigraphy of Upper Callovian–Lower Berriasian successions from Southern Alps, North Italy. Rivista Italiana di Paleontologia e Stratigrafia.
- Channell, J.E.T., 1996. Palaeomagnetism and palaeogeography of Adria. In: Morris, A., Tarling, D.H. (Eds.), Palaeomagnetism and Tectonics of the Mediterranean Region: Geological Society Special Publication, vol. 105, pp. 119–132.
- Channell, J.E.T., Erba, E., 1992. Early Cretaceous polarity chronos CM0 to CM11 recorded in northern Italian sections near Brescia. Earth and Planetary Science Letters 108, 161–179.
- Channell, J.E.T., Grandesso, P., 1987. A revised correlation of Mesozoic polarity chronos and calpionellid zones. Earth and Planetary Science Letters 85, 222–240.
- Channell, J.E.T., D'Argenio, B., Horvath, F., 1979a. Adria, the African promontory, in Mesozoic mediterranean paleogeography. Earth Science Reviews 15, 213–292.
- Channell, J.E.T., Lowrie, W., Medizza, F., 1979b. Middle and Early Cretaceous magnetic stratigraphy from the Cisson section, Northern Italy. Earth and Planetary Science Letters 42, 153–166.

- Channell, J.E.T., Bralower, T.J., Grandesso, P., 1987. Biostratigraphic correlation of M-sequence chronos CM1 to CM23 at Capriolo and Xausa (S. Alps, Italy). *Earth and Planetary Science Letters* 85, 203–221.
- Channell, J.E.T., Doglioni, C., Stoner, J.S., 1992. Jurassic and Cretaceous paleomagnetic data from the Southern Alps (Italy). *Tectonics* 11, 811–822.
- Channell, J.E.T., Erba, E., Lini, A., 1993. Magnetostratigraphic calibration of the Late Valanginian carbon isotope event in pelagic limestones from Northern Italy and Switzerland. *Earth and Planetary Science Letters* 118, 145–166.
- Channell, J.E.T., Erba, E., Nakanishi, M., Tamaki, K., 1995a. Late Jurassic–Early Cretaceous timescales and oceanic magnetic anomaly block models. In: Berggren, W.A., Kent, D.V., Aubry, M., Hardenbol, J. (Eds.), *Geochronology, Time Scales and Stratigraphic Correlation: SEPM Special Publication*, vol. 54, pp. 51–63.
- Channell, J.E.T., Cecca, F., Erba, E., 1995b. Correlations of Hauterivian and Barremian (Early Cretaceous) stage boundaries to polarity chronos. *Earth and Planetary Science Letters* 134, 125–140.
- Channell, J.E.T., Erba, E., Muttoni, G., Tremolada, F., 2000. Early Cretaceous magnetic stratigraphy in the APTICORE drill core and adjacent outcrop at Cismon (Southern Alps, Italy), and correlation to the proposed Barremian/Aptian boundary stratotype. *Geological Society of America Bulletin* 112, 1430–1443.
- Chiari, M., Cobianchi, M., Picotti, V., 2007. Integrated stratigraphy (radiolarians and calcareous nannofossils) of the Middle to Upper Jurassic alpine Radiolarites (Lombardian Basin, Italy): constraints to their genetic interpretation. *Palaeogeography, Palaeoclimatology, Palaeoecology* 249 (3–4), 233–270.
- Cobianchi, M., 1992. Sinemurian–Early Bajocian calcareous nannofossil biostratigraphy of the Lombardy Basin (Southern calcareous Alps, Northern Italy). *Atti Ticinensi di Scienze della Terra* 35, 61–106.
- De Kaenel, E., Bergen, J.A., Perch-Nielsen, K., 1996. Jurassic calcareous nannofossil biostratigraphy of Western Europe. Compilation of recent studies and calibration of bioevents. *Bulletin de la Societe Geologique de France* 167 (1), 15–28.
- Eby, G.N., Krueger, H.M., Creasy, J.W., 1992. Geology, geochronology, and geochemistry of the White Mountain batholith, New Hampshire. In: Puffer, J.H., Ragland, P.C. (Eds.), *Eastern North American Mesozoic Magmatism: Geol. Soc. America, Special Paper*, 268, pp. 379–397.
- Erba, E., 2004. Calcareous nannofossils and Mesozoic oceanic anoxic events. *Marine Micropaleontology* 52, 85–106.
- Erba, E., Quadrio, B., 1987. Biostratigrafia a Nannofossili calcarei, Calpionellidi e Foraminiferi planctonici della Maiolica (Titoniano superiore–Aptiano) nelle Prealpi Bresciane (Italia settentrionale). *Rivista Italiana di Paleontologia e Stratigrafia* 93 (1), 3–108.
- Erba, E., Channell, J.E.T., Claps, M., Jones, C., Larson, R., Opdyke, B., Premoli-Silva, I., Riva, A., Salvini, G., Torricelli, S., 1999. Integrated stratigraphy of the Cismon APTICORE (Southern Alps, Italy): a “reference section” for the Barremian–Aptian interval at low latitudes. In: Huber, B., Bralower, T.J., Leckie, R.M. (Eds.), *Biotic Change and Paleoenvironment of Black Shale Environments – A memorial to William V. Sliter: Journal Foraminiferal Research*, vol. 29, pp. 371–391.
- Gaetani, M., Poliani, G., 1978. Il Toarciano e il Giurassico medio in Albenza (Bergamo). *Rivista Italiana di Paleontologia e Stratigrafia* 84 (2), 349–382.
- Gradstein, F.M., Ogg, J.G., Smith, A.G., 2004. *A Geologic Time Scale*. Cambridge University Press. [589 pp.]
- Hargraves, R.B., 1989. Palaeomagnetism of Mesozoic kimberlites in southern Africa and the Cretaceous apparent polar wander curve for Africa. *Journal of Geophysical Research* 94, 1851–1866.
- Hargraves, R.B., Briden, J.C., Daniels, B.A., 1999. Palaeomagnetism and magnetic fabric in the Freetown Complex, Sierra Leone. *Geophysical Journal International* 136, 705–713.
- Hinnov, L.A., Park, J., 1999. Strategies for assessing Early–Middle (Pliensbachian–Aalenian) Jurassic cyclochronologies. In: Shackleton, N.J., Mc Cave, I.N., Weedon, G.P. (Eds.), *A Discussion: Astronomical (Milankovitch) Calibration of the Geological Timescale: Philosophical Transactions of the Royal Society, London, Series A*, vol. 357, pp. 1831–1859.
- Hinnov, L.A., Park, J., Erba, E., 2000. Lower–Middle Jurassic rhythmites from the Lombard Basin, Italy: a record of orbitally forced carbonate cycles modulated by secular environmental changes in West Tethys. In: Hall, R.L., Smith, P.L. (Eds.), *Advances in Jurassic Research: Trans Tech Publications*, pp. 437–454.
- Horner, F., Heller, F., 1983. Lower Jurassic magnetostratigraphy at the Breggia Gorge (Ticino, Switzerland) and Alpe Turati (Como, Italy). *Geophysical Journal of the Royal Astronomical Society* 73, 705–713.
- Kirschvink, J.L., 1980. The least squares lines and plane analysis of paleomagnetic data. *Geophysical Journal of the Royal Astronomical Society* 62, 699–718.
- Klitgord, K.D., Schouten, H., 1986. Plate kinematics of the central Atlantic. In: Vogt, P.R., Tuchocke, B.E. (Eds.), *The Western North Atlantic Region, The Geology of North America, M: Geological Society of America*, pp. 351–378.
- Martire, L., 1996. Stratigraphy, facies and synsedimentary tectonics in the Jurassic Rosso Ammonitico Veronese (Altopiano di Asiago, NE Italy). *Facies* 35, 209–236.
- Martire, L., Clari, P., Lozzi, F., Pavia, G., 2006. The Rosso Ammonitico Veronese (Middle–Upper Jurassic of the Trento Plateau): a proposal of lithostratigraphic ordering and formalization. *Rivista Italiana di Paleontologia e Stratigrafia* 112 (2), 227–250.
- Mattioli, E., Erba, E., 1999. Synthesis of calcareous nannofossil events in Tethyan Lower and Middle Jurassic successions. *Rivista Italiana di Paleontologia e Stratigrafia* 105 (3), 343–376.
- Muttoni, G., Kent, D.V., Channell, J.E.T., 1996. Evolution of Pangea: paleomagnetic constraints from the Southern Alps, Italy. *Earth and Planetary Science Letters* 140, 97–112.
- Muttoni, G., Garzanti, E., Alfonsi, L., Cirilli, S., Germani, D., Lowrie, W., 2001. Motion of Africa and Adria since the Permian: paleomagnetic and paleoclimatic constraints from northern Libya. *Earth and Planetary Science Letters* 192, 159–174.
- Muttoni, G., Kent, D.V., Garzanti, E., Brack, P., Abrahamsen, N., Gaetani, M., 2003. Early Permian Pangea “B” to Late Permian Pangea “A”. *Earth and Planetary Science Letters* 215, 379–394.
- Muttoni, G., Erba, E., Kent, D.V., Bachatadse, V., 2005. Mesozoic Alpine facies deposition as a result of past latitudinal plate motion. *Nature* 434, 59–63.
- Ogg, J.G., 1981. Sedimentology and paleomagnetism of Jurassic pelagic limestones: “Ammonitico Rosso” facies. Unpublished PhD thesis, Scripps Institution of Oceanography, University of California at San Diego, 212 pp.
- Ogg, J.G., 2004. The Jurassian period. In: Gradstein, F., Ogg, J., Smith, A. (Eds.), *A Geologic Time Scale*. Cambridge University Press, pp. 307–343.
- Ogg, J.G., Hasenjäger, R.W., Wimbleton, W.A., Channell, J.E.T., Bralower, T.J., 1991. Magnetostratigraphy of the Jurassic/Cretaceous boundary interval–Tethyan and English fauna realms. *Cretaceous Research* 12, 455–482.
- Ogg, J.G., Ogg, G., Gradstein, F., 2008. *The Concise Geologic Time Scale*. Cambridge University Press. [177 pp.]
- Perch-Nielsen, K., 1985. Mesozoic calcareous nannofossils. In: Bolli, H.M., Saunders, J.B., Perch-Nielsen, K. (Eds.), *Plankton Stratigraphy*. Cambridge University Press, Cambridge, pp. 329–426.
- Satolli, S., Besse, J., Speranza, F., Calamita, F., 2007. The 125–150 Ma high-resolution Apparent Polar Wander Path for Adria from magnetostratigraphic sections in Umbria–Marche (Northern Apennines, Italy): timing and duration of the global Jurassic–Cretaceous hairpin turn. *Earth and Planetary Science Letters* 257, 329–342.
- Sichler, J.L., Olivet, J.M., Auzende, H., Jonquet, H., Bonnin, J., Bonifay, A., 1980. Mobility of Morocco. *Canadian Journal of Earth Sciences* 17, 1546–1558.
- Tauxe, L., Kent, D.V., 2004. A simplified statistical model for the geomagnetic field and the detection of shallow bias in palaeomagnetic inclinations: was the ancient magnetic field dipolar? In: Channell, J.E.T., Kent, D.V., Lowrie, W., Meert, J.G. (Eds.), *Timescales of the Palaeomagnetic Field*. American Geophysical Union, Washington, DC.
- Thierstein, H.R., 1971. Tentative Lower Cretaceous nannoplankton zonation. *Elogiae Geologicae Helvetiae* 64, 459–488.
- Thierstein, H.R., 1973. Lower Cretaceous calcareous nannoplankton biostratigraphy. *Abhandlungen der Geologischen Bundesanstalt* A29, 1–52.
- Van Fossen, M.C., Kent, D.V., 1990. High-latitude paleomagnetic poles from middle Jurassic plutons and Moat Volcanics in New England and the controversy regarding Jurassic apparent polar wander for North America. *Journal of Geophysical Research* 95, 17503–17516.
- Van Fossen, M.C., Kent, D.V., 1992. Paleomagnetism of 122 Ma plutons in new England and the Mid-Cretaceous paleomagnetic field in North America: true polar wander or large-scale differential mantle motion? *Journal of Geophysical Research* 97, 19,651–19,661.
- Van Fossen, M.C., Kent, D.V., 1993. Palaeomagnetic study of 143 Ma kimberlite dikes in central New York State. *Geophysical Journal International* 113, 175–185.
- Wiedenmayer, F., 1980. Die Ammoniten der mediterranean provinz in Pliensbachian und im unteren Toarcian aufgrund neuer Untersuchungen im Generoso–Becken (Lombardische Alpen). *Denkschrift der Schweizerischen Naturforschenden Gesellschaft*, 93, Birkhäuser, Basel, 260 pp.
- Wimbleton, W.A.P., 2009. Fixing a basal Berriasian and J/K boundary. In: Hart, M.B. (Ed.), *8th International Symposium on the Cretaceous System*, 6th–12th September, 2009, Abstract Volume, 196–198, Plymouth.
- Wimbleton, W.A.P., Casellato, C.E., Rehákova, D., Bulot, L.G., Erba, E., Gardin, S., submitted for publication. Fixing a basal Berriasian and Jurassic–Cretaceous (J–K) boundary—perhaps there is some light at the end of the tunnel? *Proceedings of the 8th International Symposium on the Cretaceous System*, 6th–12th September 2009, Plymouth. *Cretaceous Research*.
- Winterer, E.L., Bosellini, A., 1981. Subsidence and sedimentation on the Jurassic passive continental margin, Southern Alps. *American Association of Petroleum Geologists Bulletin* 65, 394–421.